Chapter 2
Charge Exchange: Atomistics

Abstract This chapter addresses primarily the process of charge exchange and cross sections for electron capture. The theory of electron loss, which is similar to the theory of target ionization, is indicated only briefly in this chapter. The treatment of charge exchange includes classical and quantal theory of the Thomas process as well as other classical models by Bohr and others. Essential steps are described in the development of the quantum theory of charge exchange for light ions, in particular problems encountered with the Brinkman-Kramers theory and the significance of first- vs. second-order perturbation theory in charge exchange. Brief accounts are given of the distorted-wave and eikonal approximations to charge exchange as well as the process of radiative electron capture. The chapter concludes with a list of data sources.

2.1 Introductory Comments

An ion penetrating through a gaseous or condensed material can experience a change in its charge by losing or capturing one or more electrons in collisions with the constituents of the medium. Such events affect the stopping and scattering of the penetrating particle and, therefore, more or less directly, the induced radiation effects.

Electron loss in a collision may be viewed as an ionization event, where the roles of the projectile and the target are interchanged. This implies that much of the theory described in other chapters of Volumes 1 and 2 of this monograph can be applied to electron loss. However, the particle that loses electrons is typically positively charged now rather than neutral. Conversely, the particle that gives rise to electron loss is a target atom which, in the context of this monograph, is most often electrically neutral.

There is no analog to electron capture in what we have looked at so far. However, the jump of an electron from one atom or ion to another one is one of the central

P. Sigmund, *Particle Penetration and Radiation Effects Volume 2*,
Springer Series in Solid-State Sciences 179, DOI: 10.1007/978-3-319-05564-0_2,

problems in many areas of science, especially in chemistry and biochemistry, plasma physics, biophysics and astrophysics.

From an atomic-collision physics point of view, a charge-exchange process between two atomic particles may be viewed from any frame of reference. In other words, the theory of the process

$$A^+ + B^0 \rightarrow A^0 + B^+ \tag{2.1}$$

is independent of whether A^+ or B^0 is viewed as the target. Therefore, in atomic-collision physics the term 'charge exchange' denotes what is called 'electron capture' in particle penetration. In particle penetration, on the other hand, 'charge exchange' denotes the exchange of an electron between the projectile and the medium, and hence the interplay of capture *and* loss of electrons by the projectile.

The phenomenon of electron capture was predicted by Flamm and Schumann (1916) and discovered experimentally by Henderson (1923) who identified the presence of He^+ ions in a beam of alpha particles penetrating through a gas. A first attempt of a theoretical explanation was made by Thomas (1927) on the basis of classical collision theory, and the quantal approach was pioneered by Oppenheimer (1928) and Brinkman and Kramers (1930).

Renewed interest in charge-changing processes in connection with particle penetration arose with the discovery of nuclear fission. Fragments from a fission reaction are fairly heavy, highly-charged ions with atomic numbers around 40 and 50, respectively, with initial velocities $v/v_0 \lesssim 10$. The importance of charge-exchange processes in the slowing down of such fragments was recognized by Bohr (1940, 1941) immediately after the discovery of fission. This was followed up in extensive measurements by Lassen (1951a,b) which were mentioned in the previous chapter.

When particle accelerators became available for atomic-physics experiments, measurements on charge exchange became a favoured subject, as is evidenced in early reviews by Allison (1958), Nikolaev (1965) and Betz (1972) that are still worthwhile reading. In the meantime the literature has exploded, but the present survey will focus on topics that are of importance in particle penetration. Amongst central theoretical references I like to mention classic papers by Thomas (1927), Brinkman and Kramers (1930), Bell (1953) and Bohr and Lindhard (1954), and more recent comprehensive reviews by Bransden and McDowell (1992), Dewangan and Eichler (1994) and Tolstikhina and Shevelko (2013).

While the theory of charge exchange is one of the most challenging areas in atomic-collision physics, a reader interested mostly in applications may jump over this chapter on first reading and return to specific sections as the need arises.

2.2 Charge-Changing Events

Let us first consider the simple case of a stripped ion, e.g., a swift proton meeting a free electron. Can the electron be captured by the proton? Well, if no other particle

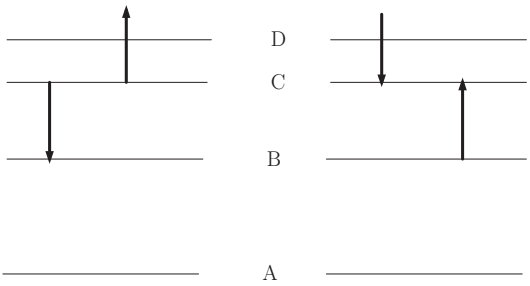

Fig. 2.1 Left: Electron emission by Auger process; right: Electron capture by inverse Auger recombination. Symbols A–D indicate energy levels

is involved, the process is forbidden by the conservation laws of energy and momentum: If it were allowed, the reverse process would likewise be allowed, where a hydrogen atom spontaneously emits its electron without any external action.

To be more precise, consider the process in the rest frame of the ion: A free electron approaching the nucleus has a positive energy, and hence will be scattered rather than captured. Hence, in order to be captured, the electron must have a way to get rid of its energy.

Let us see what happens if a third particle is involved. This could be a photon. Indeed, if the collision is accompanied by the emission of a photon, excess energy can be carried away so that the electron can end up in a bound state. This is called radiative recombination (Oppenheimer, 1928) or 'radiative electron capture' (REC). While the cross section for such a process is negligible at velocities $v \ll c$, radiative electron capture is an important process in the relativistic regime.

Restrictions imposed by conservation laws can also be overcome if the ion carries electrons to start with. The kinetic energy of the captured electron may be transmitted to one or more electrons which get excited. You may view this as an inverse Auger process. Figure 2.1(left) illustrates an Auger process, where an electron jumps from a level C to a lower level B, thereby giving its energy to another electron that can jump from level C to the continuum. The inverse process, i.e., inverse Auger recombination, is illustrated on the right diagram in Fig. 2.1.

More important in the context of particle penetration is the charge exchange between two or more atomic particles. In that case, energy and momentum conservation are taken care of primarily by the motion of the recoiling nuclei which, as a first approximation, is independent of the behaviour of the electrons. These nuclei provide a time-dependent potential that governs the motion of the electrons, somewhat similar to what happens in a molecule. In close collisions, electron orbits may even temporarily resemble those in a 'united atom', i.e., an atom with atomic number $Z_1 + Z_2$. An electron bound to one atom before a collision has a statistical chance to be bound to the other one at the time of separation. This process has high probability if it can proceed without a major change in orbital speed. Therefore, the cross section for the process decreases rapidly when the projectile speed does not match

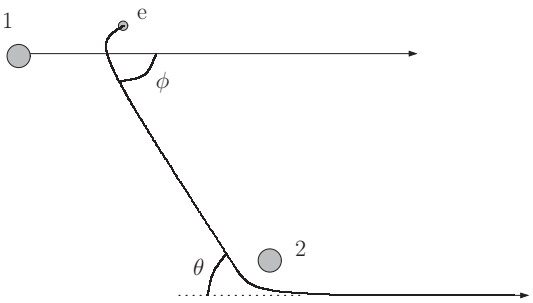

Fig. 2.2 Double-scattering process leading to electron capture according to Thomas (1927)

an orbital speed. A proper description of this type of resonant process invokes the laws of quantum mechanics.

At high relative velocities, multiple collisions between an electron and the colliding nuclei may end up with an electron bound to the projectile. This process will be discussed in the following section.

Special considerations may be necessary for particles penetrating through condensed matter, where the question of whether or not an electron is bound to a projectile may not have a unique answer. This is not only of theoretical interest: Swift ions emerging from a foil are accompanied by electrons. As mentioned in Sect. 1.5.3, the energy spectrum of these emitted 'secondary electrons' frequently shows a 'convoy peak' in the beam direction at an energy $\sim mv^2/2$, where v is the velocity of the emerging ion beam. Such convoy or 'cusp' electrons, which may reflect 'capture into continuum' or 'loss into the continuum' may have travelled in the vicinity of the ion for a certain pathlength.

In this connection an operational definition of the charge of an ion travelling through a material is needed. This may be achieved with X-ray spectroscopic methods: Since the energy of an X-ray emission line depends on the charge of the emitting atom, X-rays emitted from penetrating ions will be split into a family of satellite lines reflecting the charge states involved (Knudson et al., 1974, Horvat et al., 1995).

2.3 Early Estimates

2.3.1 Double Scattering: The Thomas Process

A simple process leading to electron capture was proposed by Thomas (1927), see Fig. 2.2. A projectile **1** moves with a speed v toward a target atom **2** and hits a target electron **e** which is kicked off with a recoil speed v_e. If the electron can be considered initially at rest, the relation between the recoil angle ϕ and the electron energy reads

$$\frac{1}{2}mv_e^2 = 2mv^2\cos^2\phi\,. \tag{2.2}$$

according to (3.7) and (3.8), Vol. 1. Hence, for $\phi = 60°$ we have

$$v_e = v\,. \tag{2.3}$$

This is a necessary condition for the electron to be captured by the projectile, but not a sufficient one, since the direction of motion does not match that of the projectile. However, if the spatial configuration allows a subsequent collision with the target nucleus, the electron may scatter another 60° with negligible energy loss. If this happens in the same scattering plane, and if the kinetic energy $mu^2/2$ in a reference frame moving with the projectile is lower than the binding energy, the electron can be considered as being captured.

Up to this point the argument rests on conservation laws of energy and momentum and is, therefore, independent of whether a classical or quantal description is adopted. When it comes to the evaluation of the cross section, there is, however, a difference. Thomas (1927) evaluated a cross section for this process on the basis of classical collision theory. His derivation hinges heavily on the relation between impact parameter and scattering angle for the two consecutive collisions. The neglect of the orbital motion implies that the theory can only be valid for $v \gg v_0$. In that velocity range a classical description of electron motion becomes questionable according to Sect. 2.3.6, Vol. 1. The predicted capture cross section, which will not be derived here, reads

$$\sigma_c = \frac{64\sqrt{2}}{3}\pi a_0^2 Z_1^2 Z_2^{7/2} \left(\frac{a_0}{b_1}\right)^{7/2} \left(\frac{v_0}{v}\right)^{11} \tag{2.4}$$

for alpha particles in hydrogen, where $b_1 = 2Z_1e^2/mu_{\max}$ and $u_{\max}$ is the maximum allowed relative speed where the electron still is bound to the projectile.

Equation (2.4), when taken literally as *the* theory of charge exchange at high velocity, was found to predict cross sections several orders of magnitude smaller than measured. This, however, does not imply that the process does not exist:

1. The predicted velocity dependence $\propto v^{-11}$ of the capture cross section was subsequently found to describe the behaviour of the total capture cross section in the limit of high but nonrelativistic projectile speed (Drisko, 1955).
2. Despite a low *total* capture cross section the process leaves a signature in the *differential* cross section, i.e., the cross section at a given scattering angle of the projectile. Indeed, since the electron carries away a lateral momentum $mv\sin\phi$, the Thomas process should be observable at an angle

$$\theta \simeq \frac{m}{M_1}\sin\phi = \frac{\sqrt{3}}{2}\frac{m}{M_1} \tag{2.5}$$

from the incident-beam direction. This peak was found in experiments by Horsdal-Pedersen et al. (1983) on H^+-He and H^+-H_2 and by Vogt et al. (1986) on H^+-H, as is illustrated in Fig. 2.3.

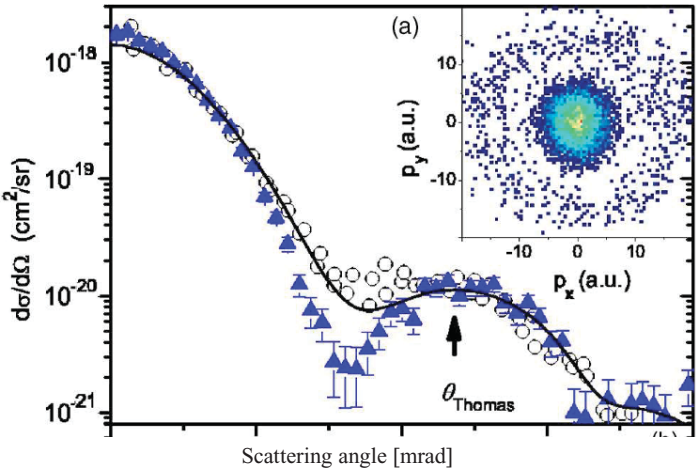

Fig. 2.3 Differential cross section for single-electron capture in 7.5 MeV H^+-He collision. Empty symbols: Measurements of Horsdal-Pedersen et al. (1983). Solid symbols: Measurements of Fischer et al. (2006). Solid line: Measurements of Fischer et al. (2006) convoluted with experimental resolution of Horsdal-Pedersen et al. (1983). From Fischer et al. (2006)

3. Double scattering processes may be treated in second-order quantal perturbation theory. Such calculations have been performed and will be discussed in Sect. 2.4.5.1.
4. Spruch (1978) demonstrated that the classical treatment of the Thomas process is valid when applied to the charge exchange between highly excited, high-angular-momentum quantum states.

2.3.2 Bohr's Model

A characteristic feature of the Thomas model is the fact that the orbital motion of the target electron in its initial state is left out of consideration in the kinematics of the capture process. Instead, the electron speed is adjusted to that of the projectile by the first of two collision events. This feature also enters into an early estimate by Bohr (1948) which, like the Thomas model, addressed electron capture by swift alpha particles. Bohr notes that the cross section for acceleration to $\sim v$ is given by

$$\sigma_v \sim \pi b^2 \tag{2.6}$$

with $b = 2Z_1 e^2/mv^2$ (cf. Problem 3.7, Vol. 1). The criterion for capture, however, is quantal and requires the electron to be confined to a sphere with a radius $a' \sim \hbar/mv$ around the projectile nucleus. The probability P for this to happen is given by the ratio $(a'/a)^3$, where $a = a_0/Z_1$ is the orbital radius in the projectile ground state, i.e.,

$$P \sim \left(\frac{Z_1 v_0}{v}\right)^3 . \tag{2.7}$$

On the basis of a simple atomic model, Bohr argued that the number of target electrons that could be captured by this process was given by

$$n \sim Z_2^{1/3} \frac{v}{v_0} . \tag{2.8}$$

Collecting these factors, Bohr obtained a capture cross section

$$\sigma_c \sim 4\pi a_0^2 Z_1^5 Z_2^{1/3} \left(\frac{v_0}{v}\right)^6 . \tag{2.9}$$

While Bohr reported reasonable agreement with early measurements on alpha-particle ranges by Rutherford (1924), we need to keep in mind that direct measurements of capture cross sections did not exist at the time of writing[1].

2.4 Quantum Theory of One-Electron Capture ⋆

2.4.1 A Qualitative Estimate

An essential feature of both the Thomas and the Bohr model is the need to *accelerate* the electron in the capture process. However, regardless of the magnitude of the projectile speed v, there is a probability for an electron in an atom to have an orbital speed v_e of the order of or even exceeding v, although this probability decreases rapidly as v exceeds the mean velocity of the tightest-bound electrons. Therefore, quantum theory allows charge exchange by a process where the electron velocity in the target frame matches an orbital velocity in the projectile.

Figure 2.4 illustrates this process in classical terms: An electron with an orbital speed v_e, bound to a target nucleus 2, has a velocity $\boldsymbol{v}_e - \boldsymbol{v}$ relative to a penetrating projectile 1. Let us assume the two nuclei to be identical, e.g. hydrogen. Then, if

$$|\boldsymbol{v}_e - \boldsymbol{v}| = v_e , \tag{2.10}$$

the electron may orbit around the projectile nucleus 1 after the collision without having to get rid of (or gain) kinetic energy.

From (2.10) you easily derive

$$\boldsymbol{v} \cdot \boldsymbol{v}_e = v^2/2 . \tag{2.11}$$

This condition can only be fulfilled if

$$v_e \geq v/2 . \tag{2.12}$$

[1] Bohr's paper, although printed in 1948, had been essentially finished about a decade earlier.

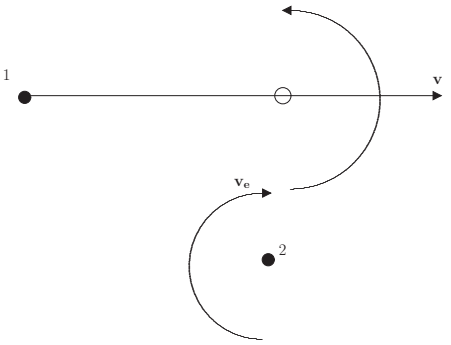

Fig. 2.4 Classical illustration of resonant electron capture. See text

Now, in classical mechanics, orbital radius and speed are uniquely related by Kepler's third law. Therefore this process is only possible for a distinct configuration in space (impact parameter) and time. In quantum mechanics the uncertainty principle allows these conditions to relax. We may then estimate a capture cross section

$$\sigma_c \propto \pi r_0^2 P_1(v/2) P_2(v/2), \,, \tag{2.13}$$

where

$$P_2(v/2) = \int_{v_e > v/2} \mathrm{d}^3 \boldsymbol{v}_e f_2(\boldsymbol{v}_e) \,, \tag{2.14}$$

is the probability for a target electron to have an orbital speed exceeding $v/2$. Here $f_2(\boldsymbol{v}_e)$ is the velocity distribution in the initial state, $P_1(v/2)$ is the analog of $P_2(v/2)$ for the projectile, and

$$r_0(v) \sim \frac{2\hbar}{v} \tag{2.15}$$

is a representative radius defining the area in which capture is possible.

For $Z_1 = Z_2$ and hydrogenic $1s$ wave functions with a screening radius a you may like to estimate the probability $P_2(v/2)$ in Problem 2.4. For $v \gg v_0/Z$ you find

$$P_2(v/2) = \frac{4}{5\pi} \left(\frac{a_0 v_0}{a v} \right)^5 \,. \tag{2.16}$$

With this, (2.13) reduces to

$$\sigma_c \sim \frac{2^{22}}{25\pi} a_0^2 Z^{10} \left(\frac{v_0}{v} \right)^{12} \,. \tag{2.17}$$

Apart from a numerical factor, this is identical with the result of the rigorous quantal calculation by Brinkman and Kramers (1930) which will be sketched below.

Note distinctly different dependencies on the projectile speed v in (2.4), (2.9) and (2.17), providing stringent experimental tests on existing theories.

2.4.2 General Considerations

We shall now have a look at charge exchange from a similar starting point as in Sect. 4.3, Vol. 1, where the Bethe theory of excitation and energy loss was presented on the basis of quantal perturbation theory. Charge exchange is more complex, since the initial and final wave functions belong to different basis sets generated by different hamiltonians, dependent on whether it is the target or the projectile that binds an electron.

Unlike the Bethe theory which, in its original form, is still today a quantitative tool in the description of stopping for a considerable fraction of the pertinent parameter space in particle penetration, the original theory of charge exchange, initiated by Oppenheimer (1928) and Brinkman and Kramers (1930), encountered unexpected problems, the solution of which turned out to be a longlasting, somewhat painful but also illuminating process. You may find a clear and encyclopedic description of this development, summarizing contributions from over 400 references to the pertinent literature, in a review by Dewangan and Eichler (1994). The discussion in the following two sections relies heavily on this work, but I shall shortcut the historical development and try to arrive at the simplest conclusions more or less directly, still following Dewangan and Eichler (1994) in numerous details.

The notation in this chapter will be more similar to the one adopted in Volume 1 than to the standard notation that has developed in the literature on charge exchange over the years.

2.4.3 Semiclassical Theory

We shall consider a three-particle system consisting of a target nucleus with atomic number Z_2 located in the origin, a projectile nucleus with atomic number Z_1 in uniform motion,

$$\boldsymbol{R}(t) = \boldsymbol{p} + \boldsymbol{v}t\,, \tag{2.18}$$

and an electron bound initially to the target nucleus. Equeation (2.18) implies that we operate in the semiclassical (or impact-parameter) picture. You may recall from Sects. 4.3 and 4.4, Vol. 1 that apart from terms of the order of m/M_1 and m/M_2, the semiclassical picture delivers the same excitation cross sections as a fully quantal description involving an incident plane wave. The same can be shown to be true in charge exchange (Crothers and Holt, 1966, Dewangan and Eichler, 1994) but will not be detailed here.

2.4.3.1 The Hamiltonian

The hamiltonian of the system may be written in the form

$$\mathcal{H} = \frac{p^2}{2m} + V_2(r) + V_1(|\boldsymbol{r} - \boldsymbol{R}|) + V_{12}(R)\,, \tag{2.19}$$

where

$$V_2(r) = -\frac{Z_2 e^2}{r}; \quad V_1(|\boldsymbol{r} - \boldsymbol{R}|) = -\frac{Z_1 e^2}{|\boldsymbol{r} - \boldsymbol{R}|}; \quad V_{12}(R) = \frac{Z_1 Z_2 e^2}{R}\,. \tag{2.20}$$

The interaction potential $V_{12}(R)$ between the nuclei does not produce a force on the electron, but it has been included nevertheless because it depends on time through $R(t)$. The kinetic energy of the projectile nucleus, on the other hand, is taken constant here and can, therefore, safely be neglected.

In the absence of the projectile, electron motion is governed by the hamiltonian

$$H = \frac{p^2}{2m} + V_2(r) \tag{2.21}$$

with eigenstates $u_j(\boldsymbol{r})$ and energies ϵ_j.

We now split the hamiltonian $\mathcal{H}$ according to

$$\mathcal{H} = \mathcal{H}_2 + \mathcal{V}_1\,, \tag{2.22}$$

where

$$\mathcal{H}_2 = H + V_{12}(R) + V_1(R) \tag{2.23}$$

and

$$\mathcal{V}_1 = V_1(|\boldsymbol{r} - \boldsymbol{R}|) - V_1(R)\,. \tag{2.24}$$

Here, a term $V_1(R)$ has been added to the unperturbed hamiltonian and subtracted from the perturbation. This innocently-looking step was first proposed by Bates (1958), but it was Cheshire (1964) who recognized its central significance. Since it causes the perturbation $\mathcal{V}_1$ to decrease as R^{-2} for large R, it removes undesired consequences of the long range of the Coulomb force of the type encountered in Sect. 3.5.1, Vol. 1.

2.4.3.2 Unperturbed Wave Functions

Let us first determine the unperturbed eigenstates of

$$\mathcal{H}_2 = H + f(t) \tag{2.25}$$

with

$$f(t) = V_{12}(R) + V_1(R) = \frac{Z_1(Z_2 - 1)e^2}{R}\,. \tag{2.26}$$

Since $f(t)$ does not contain the electron coordinate $\boldsymbol{r}$, it will make itself noticed as a phase factor $\mathrm{e}^{-\mathrm{i}\alpha(t)}$ in the wave function with

$$\alpha(t) = \frac{1}{\hbar}\int^t \mathrm{d}t'\, f(t') = \frac{1}{\hbar}\int^t \mathrm{d}t'\, \frac{Z_1(Z_2-1)e^2}{\sqrt{p^2+(vt')^2}} \tag{2.27}$$

or

$$\alpha(t) = -\nu_1 \ln\frac{R-vt}{p} + \alpha_0\,, \tag{2.28}$$

where

$$\nu_1 = \frac{Z_1(Z_2-1)e^2}{\hbar v}\,, \tag{2.29}$$

and α_0 is an arbitrary constant which can be set equal to zero.

With this, eigenstates to $\mathcal{H}_2$ may be written as

$$\psi_j(\boldsymbol{r},t) = \mathrm{e}^{\mathrm{i}\nu_1 \ln[(R-vt)/p]}\mathrm{e}^{-\mathrm{i}\epsilon_j t/\hbar}u_j(\boldsymbol{r})\,. \tag{2.30}$$

Although we are now ready in principle to perform a perturbation expansion in terms of $\mathcal{V}_1$, we need a valid description of the end configuration, where the electron is bound to the projectile. To this end we split the hamiltonian according to

$$\mathcal{H} = \mathcal{H}_1 + \mathcal{V}_2\,, \tag{2.31}$$

where

$$\mathcal{H}_1 = \frac{p^2}{2m} + V_1(|\boldsymbol{r}-\boldsymbol{R}|) + V_{12}(R) + V_2(R) \tag{2.32}$$

and

$$\mathcal{V}_2 = V_2(r) - V_2(R)\,, \tag{2.33}$$

in strict analogy to (2.22)–(2.24).

Denoting eigenstates and energies of an electron in a projectile atom at rest as $v_\ell(\boldsymbol{r})$ and η_ℓ, respectively, an alternative basis set for the entire three-body system, making reference to bound projectile states, reads

$$\chi_\ell(\boldsymbol{r},t) = \mathrm{e}^{\mathrm{i}\nu_2 \ln[(R-vt)/p]}\mathrm{e}^{-\mathrm{i}\eta_\ell t/\hbar}v_\ell(\boldsymbol{r}-\boldsymbol{R})\,\mathrm{e}^{\mathrm{i}(\boldsymbol{k}\cdot\boldsymbol{r}-\omega t)}\,, \tag{2.34}$$

where

$$\nu_2 = \frac{Z_2(Z_1-1)e^2}{\hbar v}\,. \tag{2.35}$$

The last factor in (2.34) accounts for the uniform motion of the projectile. You may verify in problem 2.1 that

$$\hbar\boldsymbol{k} = m\boldsymbol{v}; \quad \hbar\omega = mv^2/2\,. \tag{2.36}$$

2.4.3.3 Transition Amplitude

Since the $\chi_\ell(\boldsymbol{r},t)$ form a complete basis set for the hamiltonian $\mathcal{H}$, they can serve as a basis for expansion of the exact wave function $\psi(\boldsymbol{r},t)$ of the system,

$$\psi(\boldsymbol{r},t) = \sum_{\ell} c_\ell(t)\, \chi_\ell(\boldsymbol{r},t) \tag{2.37}$$

with coefficients

$$c_\ell(t) = \int \mathrm{d}^3\boldsymbol{r}\; \chi_\ell^*(\boldsymbol{r},t)\, \psi(\boldsymbol{r},t) \tag{2.38}$$

which, in addition to time, depend on velocity $\boldsymbol{v}$ and impact parameter $\boldsymbol{p}$. The probability for the electron to be bound to the projectile into a state ℓ after the collision is given by

$$P_\ell(\boldsymbol{p},\boldsymbol{v}) = |c_\ell(\infty)|^2 \ . \tag{2.39}$$

We may write the transition amplitude in the form

$$c_\ell(\infty) = \int_{-\infty}^{+\infty} \mathrm{d}t\, \frac{\mathrm{d}}{\mathrm{d}t} \int \mathrm{d}^3\boldsymbol{r}\; \chi_\ell^*(\boldsymbol{r},t)\psi(\boldsymbol{r},t)\,, \tag{2.40}$$

since the overlap integral between the unperturbed initial target state and the unperturbed final projectile state, both taken at $t = -\infty$, vanishes.

You may rewrite the time derivative making use of the Schrödinger equation, noting that $\psi(\boldsymbol{r},t)$ is governed by $\mathcal{H}$ and $\chi_\ell(\boldsymbol{r},t)$ by $\mathcal{H}_1$,

$$\begin{aligned} c_\ell(\infty) &= \frac{1}{\mathrm{i}\hbar} \int_{-\infty}^{+\infty} \mathrm{d}t \int \mathrm{d}^3\boldsymbol{r}\; \chi_\ell^*(\boldsymbol{r},t)(\mathcal{H}-\mathcal{H}_1)\psi(\boldsymbol{r},t) \\ &= \frac{1}{\mathrm{i}\hbar} \int_{-\infty}^{+\infty} \mathrm{d}t \int \mathrm{d}^3\boldsymbol{r}\; \chi_\ell^*(\boldsymbol{r},t)\mathcal{V}_2\psi(\boldsymbol{r},t). \end{aligned} \tag{2.41}$$

If you miss some details in this derivation, go to Problem 2.2.

2.4.3.4 Perturbation Expansion

Equation (2.41) is an exact relationship. In order to determine $c_\ell(\infty)$ we need to find the function $\psi(\boldsymbol{r},t)$, which is a solution to the Schrödinger equation for the three-particle system. An impressive arsenal of theoretical/computational methods has become available for this purpose (Bransden and McDowell, 1992, Dewangan and Eichler, 1994). Here we apply a perturbation expansion in powers of $\mathcal{V}_1$ which, according to (4.36)–(4.38), Vol. 1 can be written in the form

$$\psi(\boldsymbol{r},t) = \psi_0(\boldsymbol{r},t) + \sum_j d_j^{(1)}(t)\psi_j(\boldsymbol{r},t) + \ldots \tag{2.42}$$

with

$$d_j^{(1)}(t) = \frac{1}{\mathrm{i}\hbar} \int_{-\infty}^{t} \mathrm{d}t' \int \mathrm{d}^3\boldsymbol{r}\; \psi_j^*(\boldsymbol{r},t')\mathcal{V}_1(\boldsymbol{r},t')\psi_0(\boldsymbol{r},t')\,. \tag{2.43}$$

With this we find

$$c_\ell(\infty) = c_\ell^{(1)}(\infty) + c_\ell^{(2)}(\infty)\ldots\,, \tag{2.44}$$

where

$$c_\ell^{(1)}(\infty) = \frac{1}{\mathrm{i}\hbar}\int_{-\infty}^{+\infty} \mathrm{d}t \int \mathrm{d}^3\boldsymbol{r}\; \chi_\ell^*(\boldsymbol{r},t)\mathcal{V}_2\psi_0(\boldsymbol{r},t) \tag{2.45}$$

and

$$c_\ell^{(2)}(\infty) = -\frac{1}{\hbar^2}\sum_j \int_{-\infty}^{\infty} \mathrm{d}t \int \mathrm{d}^3\boldsymbol{r}\; \chi_\ell^*(\boldsymbol{r},t)\mathcal{V}_2(\boldsymbol{r},t)\psi_j(\boldsymbol{r},t) \int_{-\infty}^{t} \mathrm{d}t' \int \mathrm{d}^3\boldsymbol{r}'\, \psi_j^*(\boldsymbol{r}',t')\mathcal{V}_1(\boldsymbol{r}',t')\psi_0(\boldsymbol{r}',t'). \tag{2.46}$$

While evaluating the leading term $c_\ell^{(1)}(\infty)$ is by no means trivial, the form of the second term indicates that the analytical complexity will increase rapidly with increasing order.

2.4.4 First-Order Perturbation

Ignoring the second-order term for a while let us focus on the first-order term

$$\psi(\boldsymbol{r},t) \simeq \psi_0(\boldsymbol{r},t)\,, \tag{2.47}$$

where $n = 0$ denotes the initial state, so that

$$c_\ell(\infty) = \frac{1}{\mathrm{i}\hbar}\int_{-\infty}^{+\infty} \mathrm{d}t \int \mathrm{d}^3\boldsymbol{r}\; \chi_\ell^*(\boldsymbol{r},t)\left(\frac{Z_2e^2}{R(t)} - \frac{Z_2e^2}{r}\right)\psi_0(\boldsymbol{r},t)\,. \tag{2.48}$$

This result, reflecting the B1B or 'boundary-corrected first Born approximation', was demonstrated by Dewangan and Eichler (1986) to produce results in good agreement with measurements of charge-exchange cross sections. The fact that valid predictions may emerge already from the first Born approximation was in contrast to the accepted view for many years.

You may wonder why it is the potential $\mathcal{V}_2$ that appears in the transition amplitude equation (2.41) rather than the perturbing potential $\mathcal{V}_1$. Well, the projection of ψ on χ_ℓ with ψ_j as the initial state is the same as the projection of ψ on ψ_j if χ_ℓ is the final state. If you adopt the latter description, you end up with (2.41), but with $\mathcal{V}_2$ replaced by $\mathcal{V}_1$, as you may verify by working on Problem 2.2.

Dual descriptions of scattering processes play a key role in the literature. This has given rise to a special nomenclature which, however, will not be followed here, because we are not going deeply enough into this subject matter to justify the effort.

2.4.4.1 Resonance Charge Exchange

Evaluation of the multiple integral equation (2.48) is complicated in general, but suitable tools have been developed for fully analytical evaluation in special cases, and accurate numerical evaluation in others. As an example we shall have a look at a relatively simple case, so-called resonance charge exchange, where $Z_1 = Z_2 = Z$ and charge exchange is considered between equivalent levels $0 \rightarrow 0$. Then, by insertion of (2.34), (2.48) reduces to

$$c_0(\infty) = \frac{1}{\mathrm{i}\hbar} \int_{-\infty}^{\infty} \mathrm{d}t \int \mathrm{d}^3\boldsymbol{r}\, \mathrm{e}^{-\mathrm{i}(\boldsymbol{k}\cdot\boldsymbol{r}-\omega t)} u_0^*(\boldsymbol{r}-\boldsymbol{R}) \left(\frac{Ze^2}{R} - \frac{Ze^2}{r}\right) u_0(\boldsymbol{r})\,, \quad (2.49)$$

where the t-dependent phase factors $\alpha(t)$ have dropped out. Now, since

$$\left(-\frac{\hbar^2}{2m}\nabla^2 - \frac{Z_2 e^2}{r}\right) u_0(\boldsymbol{r}) = \epsilon_0 u_0(\boldsymbol{r})\,, \quad (2.50)$$

where ϵ_0 is the energy of the initial (and final) state we may replace

$$\left(\frac{Ze^2}{R} - \frac{Ze^2}{r}\right) u_0(\boldsymbol{r}) = \left(\frac{Ze^2}{R} + \epsilon_0 + \frac{\hbar^2}{2m}\nabla^2\right) u_0(\boldsymbol{r})\,. \quad (2.51)$$

After introduction of the Fourier transform

$$u_0(\boldsymbol{r}) = \frac{1}{(2\pi)^{3/2}} \int \mathrm{d}^3\boldsymbol{q}\, u_0(\boldsymbol{q}) \mathrm{e}^{\mathrm{i}\boldsymbol{q}\cdot\boldsymbol{r}} \quad (2.52)$$

you find

$$c_0(\infty) = \frac{1}{(2\pi)^3 \mathrm{i}\hbar} \int_{-\infty}^{\infty} \mathrm{d}t \int \mathrm{d}^3\boldsymbol{r} \int \mathrm{d}^3\boldsymbol{q} \int \mathrm{d}^3\boldsymbol{q}' \mathrm{e}^{-\mathrm{i}(\boldsymbol{k}\cdot\boldsymbol{r}-\omega t)} \times \mathrm{e}^{-\mathrm{i}\boldsymbol{q}'\cdot(\boldsymbol{r}-\boldsymbol{R})} u_0^*(\boldsymbol{q}') \left(\frac{Ze^2}{R} + \epsilon_0 + \frac{\hbar^2}{2m}\nabla^2\right) u_0(\boldsymbol{q}) \mathrm{e}^{\mathrm{i}\boldsymbol{q}\cdot\boldsymbol{r}}. \quad (2.53)$$

Here you may carry out the ∇^2-operation and integrate over $\boldsymbol{r}$. As a result you will identify a Dirac function $\delta(-\boldsymbol{k} - \boldsymbol{q}' + \boldsymbol{q})$. After integration over $\boldsymbol{q}'$ you then arrive at

$$c_0(\infty) = \frac{1}{\mathrm{i}\hbar} \int_{-\infty}^{\infty} \mathrm{d}t\, \mathrm{e}^{\mathrm{i}\omega t} \int \mathrm{d}^3\boldsymbol{q} \times \mathrm{e}^{\mathrm{i}(\boldsymbol{q}-\boldsymbol{k})\cdot\boldsymbol{R}}\, u_0^*(\boldsymbol{q}-\boldsymbol{k}) \left(\frac{Ze^2}{R} + \epsilon_0 - \frac{\hbar^2 q^2}{2m}\right) u_0(\boldsymbol{q}). \quad (2.54)$$

2.4.4.2 Brinkman-Kramers Approximation

Recalling that R depends on time, cf. (2.18), you will find it reasonable to split (2.54) into two,

$$c_0(\infty) = c_0^{\mathrm{BK}}(\infty) + \Delta c_0(\infty)\,, \tag{2.55}$$

where $c_0^{\mathrm{BK}}(\infty)$ originates in the term $\epsilon_0 - \hbar^2 q^2/2m$ and $\Delta c_0(\infty)$ in Ze^2/R. The superscript 'BK' stands for Brinkman-Kramers[2]. Considering the former term we may integrate over time and obtain

$$c_0^{\mathrm{BK}}(\infty) = \int \mathrm{d}^3\boldsymbol{q}\; \mathrm{e}^{\mathrm{i}(\boldsymbol{q}-\boldsymbol{k})\cdot\boldsymbol{p}}\; \delta(\boldsymbol{q}\cdot\boldsymbol{v} - \boldsymbol{k}\cdot\boldsymbol{v} + \omega)\; f_0(\boldsymbol{q}) \tag{2.56}$$

with

$$f_0(\boldsymbol{q}) = \frac{2\pi}{\mathrm{i}\hbar}\, u_o^*(\boldsymbol{q}-\boldsymbol{k}) \left(\epsilon_0 - \frac{\hbar^2 q^2}{2m}\right) u_0(\boldsymbol{q}). \tag{2.57}$$

In the original work of Oppenheimer (1928) and Brinkman and Kramers (1930), the term $\Delta c_0(\infty)$ was absent. If we ignore it for a moment we may go over to the cross section

$$\sigma_0^{\mathrm{BK}} = \int \mathrm{d}^2\boldsymbol{p}\; \left|c_0^{\mathrm{BK}}(\infty)\right|^2 \tag{2.58}$$

or, after insertion of (2.56) and integration over $\boldsymbol{p}$,

$$\sigma_0 = \frac{(2\pi)^2}{v} \int \mathrm{d}^3\boldsymbol{q}\; \delta(\boldsymbol{q}\cdot\boldsymbol{v} - \boldsymbol{k}\cdot\boldsymbol{v} + \omega)\, |f_0(\boldsymbol{q})|^2 \tag{2.59}$$

according to a procedure which was used in Sect. 4.3.4, Vol. 1.

Noting first that $\omega - \boldsymbol{k}\cdot\boldsymbol{v} = -\hbar k^2/2m$ we recognize that the Dirac function under the integral implies that $\boldsymbol{q}\cdot\boldsymbol{k} = k^2/2$ and thus,

$$(\boldsymbol{q}-\boldsymbol{k})^2 = q^2. \tag{2.60}$$

Since $\hbar\boldsymbol{q}$ is the initial momentum of the target electron and $\hbar(\boldsymbol{q}-\boldsymbol{k})$ the final momentum of the captured electron seen from the laboratory frame, we learn from (2.60) that charge exchange in this model is only possible in case of exact velocity-matching. This is a quantification of the process sketched in Sect. 2.4.1, in particular Fig. 2.4. Note the equivalence of (2.60) with (2.10).

Equation (2.60) also tells us that for s-states, all angular dependence is contained in the Dirac function. Integration over the angular variable then leads to

[2] In the literature, the term OBK, which stands for Oppenheimer-Brinkman-Kramers, occurs frequently instead of BK. Both schemes, Oppenheimer (1928) and Brinkman and Kramers (1930) operate in the first Born approximation without the term Ze^2/R in the brackets, and in both schemes, (2.49) plays a central role, although Oppenheimer (1928) derived it from the plane-wave Born approximation, while Brinkman and Kramers (1930) started from the semiclassical impact-parameter description. However, while the explicit evaluation by Brinkman and Kramers (1930) involves exact integrations as described below, the evaluation by Oppenheimer (1928) invokes approximations which lead to drastic discrepancies.

$$\sigma_0^{\mathrm{BK}} = \frac{(2\pi)^5}{\hbar^2 v^2} \int_{k/2}^{\infty} q \, \mathrm{d}q \, |u_0(q)|^4 \left(\epsilon_0 - \frac{\hbar^2 q^2}{2m} \right)^2 . \tag{2.61}$$

For the $1s$ state of a hydrogen-like atom with

$$u_0(\boldsymbol{r}) = \frac{1}{\sqrt{\pi a^3}} e^{-r/a} \tag{2.62}$$

you may derive (Problem 2.3) the particularly simple result

$$\sigma_0^{\mathrm{BK}} = \pi a_0^2 2^8 \frac{v_0^2}{v^2} \int_{q=k/2}^{\infty} \frac{\mathrm{d}(qa)^2}{(1+q^2a^2)^6} \tag{2.63}$$

or, after integration,

$$\sigma_0^{\mathrm{BK}} = \pi a_0^2 \frac{2^{18} Z^{10} v_0^{12}}{5v^2(v^2+4Z^2v_0^2)^5} . \tag{2.64}$$

For $v \gg 2Z_2 v_0$ this result differs from the qualitative estimate (2.17) by a factor of $5\pi^2/16 = 3.1$. As we shall learn shortly, (2.64) predicts a too large value, and (2.17) comes closer to the correct result.

From a physical point of view, the steep decrease of the capture cross section with increasing projectile speed reflects the fact that the process involves exclusively the far tails of the velocity distribution of the electron in the target and projectile state.

This calculation can be generalized to capture into an excited state with the principal quantum number $n > 1$. For a one-electron system with arbitrary Z_1, Z_2 one finds (McDowell and Coleman, 1970)

$$\sigma_n^{\mathrm{BK}} = \pi a_0^2 \frac{2^{18}(Z_1Z_2)^5 v^8 v_0^{12}}{5n^3 \left[v^4 + 2(Z_2^2 + Z_1^2/n^2)v^2v_0^2 + (Z_2^2 - Z_1^2/n^2)^2 v_0^4 \right]^5} . \tag{2.65}$$

Setting $Z_1 = Z_2$ you may recognize that the cross section for capture into excited states falls off approximately as n^{-3}.

2.4.4.3 Relativity

Equation (2.64) experiences a major change at beam velocities approaching the velocity of light (Mittleman, 1964, Shakeshaft, 1979, Moiseiwitsch, 1980, Bransden and McDowell, 1992). Calculations on the basis of the Dirac equation show a difference between charge exchange with and without spinflip, which increases with increasing energy up to a factor of ~ 4 in the extreme relativistic regime. Available analytic estimates are based on approximations valid in the moderately relativistic range and differ from author to author. Moiseiwitsch (1980) reports capture cross sections which can be written in the form

$$\sigma_{c,\mathrm{direct}} = \frac{2^7\pi}{5} a_0^2 \frac{\alpha^{12}}{\gamma - 1} \left(\frac{\gamma + 1}{\gamma - 1 + 2\alpha^2} \right)^5 \tag{2.66}$$

for capture without spinflip and

$$\sigma_{c,\text{spinflip}} = \frac{2^3\pi}{5} a_0^2 \alpha^{12} \frac{(\gamma+1)^3}{(\gamma-1+2\alpha^2)^4} \tag{2.67}$$

for capture with spinflip. Here, $\alpha = v_0/c = 1/137$ is the fine structure constant and $\gamma = 1/\sqrt{1-v^2/c^2}$.

Both expressions are seen to go as $\sim 1/\gamma$ with increasing projectile energy, i.e., inversely proportional to the beam energy, in contrast to the steep decrease in the nonrelativistic limit.

While (2.66) approaches (2.64) for $v/c \ll 1$, (2.67) reads

$$\sigma_{c,\text{spinflip}} \overset{v/c\ll 1}{=} \frac{2^{10}\pi}{5} a_0^2 \alpha^4 \left(\frac{v_0^2}{v^2+4v_0^2}\right)^4 . \tag{2.68}$$

The factor α^4 makes this a very small quantity.

2.4.4.4 B1B Approximation

You may recall that (2.64) stems from ignoring the term Ze^2/R in (2.54) or (2.49). The term $\Delta c_0(\infty)$ in (2.55) has been evaluated by Jackson and Schiff (1953) and by Bates and Dalgarno (1952). Instead of going through a rather cumbersome integration procedure I shall try to demonstrate how it happens that incorporation of this term reduces the cross section (2.64) substantially in case of the H-H system.

For clarity, change the spatial variable in (2.49) according to $\boldsymbol{r} \to \boldsymbol{r} + \boldsymbol{R}/2$, so that

$$c_0(\infty) = \frac{1}{\mathrm{i}\hbar} \int_{-\infty}^{\infty} \mathrm{d}t\, \mathrm{e}^{-\mathrm{i}(\boldsymbol{k}\cdot\boldsymbol{R}/2+\omega t)} \int \mathrm{d}^3\boldsymbol{r}\, \mathrm{e}^{-\mathrm{i}\boldsymbol{k}\cdot\boldsymbol{r}} \\ u_0^*(\boldsymbol{r}-\boldsymbol{R}/2)\left(\frac{Ze^2}{R} - \frac{Ze^2}{|\boldsymbol{r}+\boldsymbol{R}/2|}\right) u_0(\boldsymbol{r}+\boldsymbol{R}/2), \tag{2.69}$$

Figure 2.5 shows plots of the function $u_0^*(\boldsymbol{r}-\boldsymbol{R}/2)u_0(\boldsymbol{r}+\boldsymbol{R}/2)$ for the ground state of hydrogen for $R/a = 2$ and 1/2. You may identify a horizontal ridge along the connection line between the two nuclei and otherwise a strong decrease. Taylor expansion of the factor $Ze^2/R - Ze^2/|\boldsymbol{r}+\boldsymbol{R}/2|$ around the midpoint between the nuclei, which is $\boldsymbol{r} = 0$ in (2.69), leads to

$$\frac{Ze^2}{R} - \frac{Ze^2}{|\boldsymbol{r}+\boldsymbol{R}/2|} \simeq \frac{Ze^2}{R} - \frac{2Ze^2}{R}\left(1 - 2\frac{\boldsymbol{R}\cdot\boldsymbol{r}}{R^2}\ldots\right) . \tag{2.70}$$

Here, the leading term for large R is $-1/R$. If we had failed to include the first term in (2.70), the result would have been $-2/R$ instead. Since the cross section is governed by the square of the transition amplitude, we may expect a substantial correction.

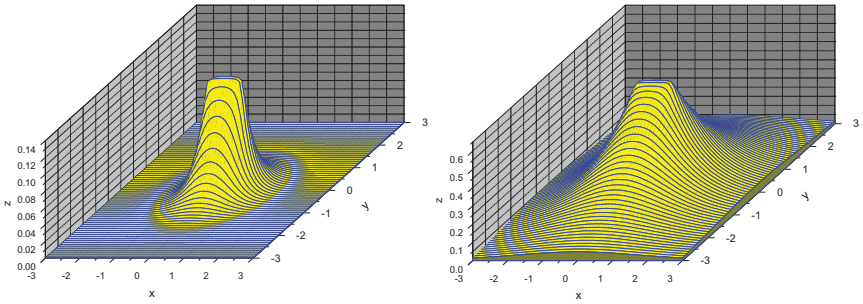

Fig. 2.5 Plots of the function $u_0^*(\boldsymbol{r} - \boldsymbol{R}/2)u_0(\boldsymbol{r} + \boldsymbol{R}/2)$ for the $1s$ state of a hydrogen-like atom. Left: $a/R = 1/2$; right: $a/R = 2$. x denotes the component of $\boldsymbol{r}$ in the direction of $\boldsymbol{R}$ in units of a. y denotes a component perpendicular to $\boldsymbol{R}$ in units of a

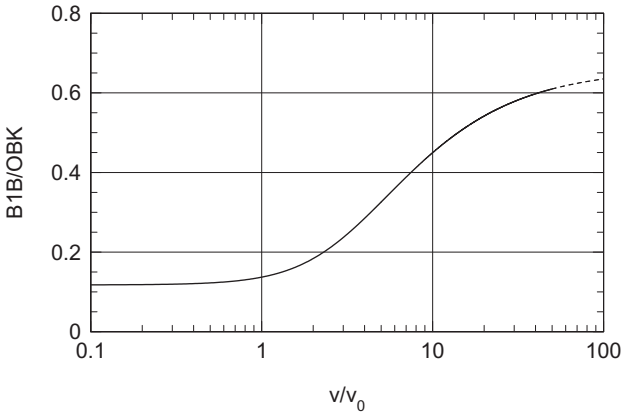

Fig. 2.6 The ratio $\sigma^{\mathrm{B1B}}/\sigma^{\mathrm{BK}}$ according to Jackson and Schiff (1953) for the H^+-H system, cf. (2.71). The dashed line indicates the regime where relativistic corrections need to be considered

According to Jackson and Schiff (1953), the ratio between the complete B1B cross section and the BK result reads

$$\frac{\sigma^{B1B}}{\sigma^{BK}} = \frac{1}{192}\left(127 + 56\frac{v_0^2}{v^2} + 32\frac{v_0^4}{v^4}\right) - \frac{1}{48}\frac{v_0}{v}\arctan\frac{v}{2v_0}\left(83 + 60\frac{v_0^2}{v^2} + 32\frac{v_0^4}{v^4}\right) + \frac{1}{24}\frac{v_0^2}{v^2}\arctan^2\frac{v}{2v_0}\left(31 + 32\frac{v_0^2}{v^2} + 16\frac{v_0^4}{v^4}\right) \quad (2.71)$$

for the H^+-H system. This function is shown in Fig. 2.6. Evidently, the B1B correction causes a decrease by up to an order of magnitude below the BK result in the pertinent velocity range $v \sim v_0$.

Relativistic calculations have been performed by Eichler (1987). For the H^+-H system, corrections to Figure 2.6 amount to a few per cent in the upper end of the graph but become very substantial for heavy ions.

2.4.4.5 Problems with the Brinkman-Kramers Approximation

For a full description of the historical development the reader is referred to the article by Dewangan and Eichler (1994). In brief, measurements on charge exchange in H^+-H collisions by Keene (1949) and Ribe (1951) demonstrated that the predictions of Brinkman and Kramers (1930) overestimated the capture cross section by about a factor of four at beam energies ranging from a few keV to over 100 keV. Almost simultaneously, Bates and Dalgarno (1952) and Jackson and Schiff (1953) pointed out that this discrepancy could be removed by adding a term e^2/R to the perturbing potential $-e^2/|\boldsymbol{r}-\boldsymbol{R}|$. The justification of this term was the fact that the hamiltonian equation (2.19) of the three-body system contains the internuclear interaction $Z_1 Z_2 e^2/R$. While it was unclear why the internuclear interaction should have such a drastic influence on the electronic transition probability, the agreement with experiment was very convincing over an energy range from $\sim$ 30 to 150 keV. It seemed plausible that poor agreement at lower velocities was due to insufficiencies of the Born approximation.

As a test of the validity of this model it was applied to heavier ions, in casu C^{6+}, N^{7+} and F^{9+} on Ar by Halpern and Law (1975). Here, cross sections calculated in the modified BK approach overestimated existing experimental values by two to three orders of magnitude. From the above derivation you may recognize that this was caused by incorporation of a term $Z_1 Z_2 e^2/R$ instead of $Z_2 e^2/R$ in the perturbation. Therefore, this extension of the Brinkman-Kramers scheme could not be taken as an acceptable solution of the charge-exchange problem.

In Sect. 2.3.1 we have seen that the Thomas capture mechanism invokes two scattering events by the electron. It seemed reasonable, therefore, to assume that a quantal description of charge exchange would warrant a treatment up to the second order in the perturbation expansion (Drisko, 1955). A wealth of clever theory has been developed based on this assumption over almost half a century, cf. the review by Dewangan and Eichler (1994). And indeed, second-order terms in the BK expansion may well be dominating over those of first order. However, once second-order terms become comparable in magnitude with first-order terms the question becomes relevant whether third- and higher-order terms ever become negligible. Indeed, even the convergence of the Born expansion itself has been questioned many years ago (Aaron et al., 1961).

It was Cheshire (1964) who identified the long range of the Coulomb interaction as the cause of the problem and who showed how to eliminate it by rearranging the hamiltonian, adding and subtracting the term $Z_2 e^2/R$. However, only H^+-H was addressed, wherewith the results of Bates and Dalgarno (1952) and Jackson and Schiff (1953) were reproduced. As a consequence, the true scope of this was only slowly recognized in the subsequent development (Belkić et al., 1979). The

breakthrough came with a paper by Dewangan and Eichler (1986) that produced a fairly reasonable description of charge exchange in the H^+-Ar system already in the first Born approximation.

2.4.4.6 Heteronuclear Systems

Electrons may be captured into a variety of final projectile states, particularly in heteronuclear collision systems, i.e., for $Z_1 \neq Z_2$, where the resonance condition $\epsilon_j = \eta_\ell$ is normally not fulfilled. Exact analytical calculations, asymptotic expansions and accurate numerical evaluations may be found in the literature, and again Bransden and McDowell (1992) and Dewangan and Eichler (1994) are very valuable sources for a literature search. Several comparisons with experimental data are shown there, which demonstrate good agreement between theory and experiment for charge exchange between bare Z_1-ions ($Z_1 > 1$) and hydrogen as well as between protons and the K-shell of an atom ($Z_2 > 1$).

Here I like to briefly discuss features that deserve attention in this context, in particular the role of the phase factor $\alpha(t)$.

Keeping within first-order perturbation theory, we may go back to (2.48) which, after insertion of (2.30) and (2.34) reads

$$c_\ell(\infty) = \frac{1}{\mathrm{i}\hbar}\int_{-\infty}^{+\infty} \mathrm{d}t \int \mathrm{d}^3\boldsymbol{r}\, \mathrm{e}^{\mathrm{i}\nu \ln[(R-vt)/p]}\, \mathrm{e}^{\mathrm{i}(\eta_\ell-\epsilon_0)t/\hbar} \times v_\ell^*(\boldsymbol{r}-\boldsymbol{R})\, \mathrm{e}^{-\mathrm{i}(\boldsymbol{k}\cdot\boldsymbol{r}-\omega t)} \left(\frac{Z_2 e^2}{R(t)} - \frac{Z_2 e^2}{r}\right) u_0(\boldsymbol{r}), \quad (2.72)$$

where

$$\nu = \nu_1 - \nu_2 = \frac{(Z_2 - Z_1)e^2}{\hbar v}. \quad (2.73)$$

You may note that the terms going as $Z_1 Z_2$, expressing the interaction $V_{12}(R)$ between the target nuclei and which enter ν_1 and ν_2, have dropped out in the difference ν. While this was to be expected, it appears gratifying nevertheless. However, a phase factor $\exp(i\,\nu \ln[|\boldsymbol{R} - \boldsymbol{v}t|/p]$ has to be dealt with for heterogeneous systems ($Z_1 \neq Z_2$). To this adds a phase factor $\exp(i\,[\eta_\ell - \epsilon_0]t/\hbar)$.

Note also that the p-dependence in (2.72) gives rise to a phase factor $\mathrm{e}^{-\mathrm{i}\nu \ln p}$. This complicates calculations on differential cross sections for charge exchange. This phase factor drops out when the capture probability $|c_\ell(\infty)|^2$ is determined, which leads to the total cross section for charge exchange.

It is of interest to study the role of the phase factor $\exp(i\,\nu \ln[(R - vt)/p])$. Figure 2.7 shows the function

$$\ln \frac{R - vt}{p} = \ln\left(\sqrt{1 + (vt/p)^2} - vt/p\right) \quad (2.74)$$

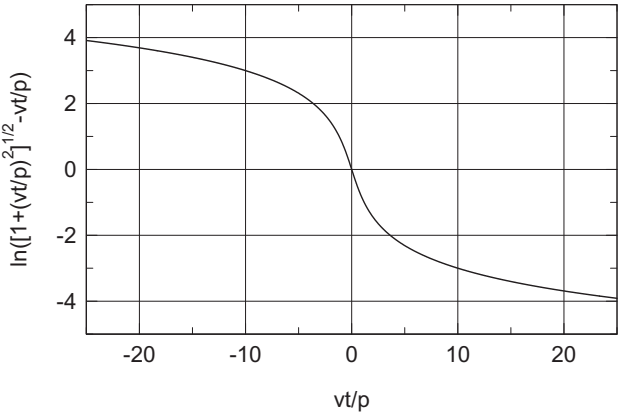

Fig. 2.7 The function $\ln(\sqrt{1+(vt/p)^2} - vt/p)$ governing the phase factor $\exp(i\nu \ln[(R - vt)/p])$ in (2.72)

versus vt/p. You may note that except in the vicinity of $t = 0$, this phase factor gives rise to rapid oscillations of the integrand, indicating that the time interval in which capture is likely, narrows in as Z_1 increases with Z_2 kept constant[3].

Figure 2.8 shows the real and imaginary part of the phase factor for $\nu = 1/2$ and 2, respectively. The theory as presented above is a high-speed theory. Hence, small values of ν appear most representative. Evidently, rapid oscillations in this case complicate the evaluation and require reliable computational methods.

2.4.5 Beyond First-Order Perturbation Theory

In addition to straight second-order perturbation theory, an impressive number of attempts has been made to explain and repair the discrepancies between calculated and measured cross sections for charge exchange. Dewangan and Eichler (1994) list and discuss twenty-one theoretical schemes. Many of them exist in a 'boundary-corrected' version, where the electron wave function carries a phase factor of the type of $\alpha(t)$, (2.28) with an arbitrary constant α_0, and an uncorrected version, where such a factor is missing. In view of the central importance of the Coulomb boundary correction, uncorrected versions may be considered inadequate, except for

[3] In the literature you will most often find a slightly different form of this phase factor, which is found by replacing p in the denominator by another constant, in casu the de Broglie wavelength $\lambda = \hbar/mv$, so that

$$\ln \frac{R - vt}{p} \to \ln \frac{mv(R - vt)}{\hbar}, \tag{2.75}$$

which is the form proposed by Cheshire (1964). This replacement reflects a different choice of the constant α_0 mentioned in (2.28) and does not affect the final result, unless an approximation is made that spoils this invariance.

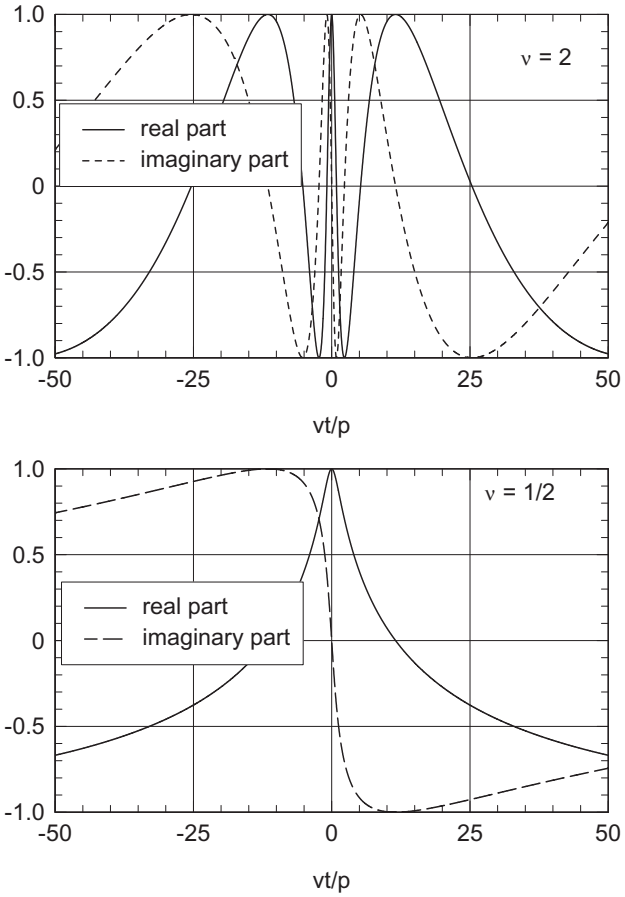

Fig. 2.8 Real and imaginary part of the phase factor $\exp(i\nu \ln[(R - vt)/p])$ entering the transition amplitude for heterogeneous collision systems, $Z_1 \neq Z_2$. Upper graph: $\nu = 2$; Lower graph: $\nu = 1/2$

$Z_1 = Z_2$, where the phase factors cancel out. Amongst eight schemes for which a boundary-corrected version exists, I wish to give preference to the CDW (continuum distorted wave) picture and the eikonal approximation.

2.4.5.1 Second-order Perturbation Theory

Contributions from second-order perturbation theory to charge exchange were discussed qualitatively right from the beginning, but interest in these contributions increased dramatically as the deficiencies of the Brinkman and Kramers (1930) approach discussed in Sect. 2.4.4.5 became evident. You may have noticed in Chaps. 3

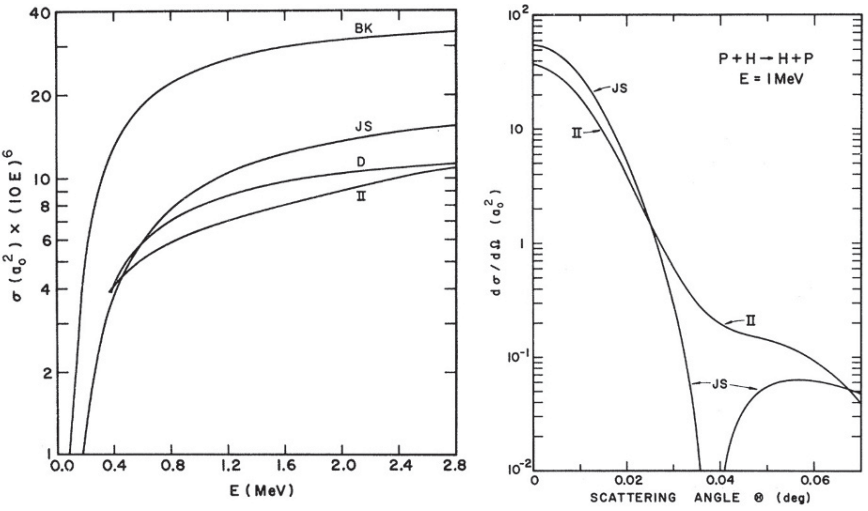

Fig. 2.9 Total (left) and differential (right) cross section for charge exchange in the H^+-H system. BK: Brinkman and Kramers (1930); JS: Jackson and Schiff (1953); D: Drisko (1955); II: Second Born approximation (Kramer, 1972); From Kramer (1972)

and 6, Vol. 1, and again in Sect. 2.4.3.4, that perturbation theory for collision processes gets considerably more complex when you go from the first to higher orders. But in hindside, the major obstacle in front of a successful theory was the lacking recognition of the Coulomb boundary condition and the importance of the rearrangement of the hamiltonian expressed by (2.22).

Early second-order theories starting with Drisko (1955), Dettmann (1971) and Kramer (1972) were straight extensions of the Brinkman-Kramers approach. Most importantly, it was found that asymptotically the contribution to the capture cross section from the second Born approximation behaved as v^{-11}, in agreement with the classical estimate of capture by double scattering (Thomas, 1927). Although the practical significance of this result is limited because relativistic corrections were neglected, it meant that first-order perturbation theory could not provide a quantitative description.

The scheme did not lead to better agreement with experimental results than the BK calculation. This led to an impressive theoretical effort by several research groups, which resulted in a variety of theoretical schemes. In addition to the distorted-wave and eikonal approximations to be sketched below, I like to mention schemes which take into account higher-order contributions in terms of either Z_1 or Z_2, whichever is bigger. Such approaches seemed appropriate for strongly asymmetric collision partners (Briggs, 1977, Macek and Shakeshaft, 1980, Macek and Taulbjerg, 1981). If you are interested in a comprehensive discussion of the pros and cons of such approaches, I refer again to Bransden and McDowell (1992) and Dewangan and Eichler (1994).

We have seen in Sect. 2.4.4.4 that the scheme of Jackson and Schiff (1953) yields results compatible with those of the B1B approximation when applied to H^+-H. From (2.46) you may extract that this feature also pertains in the second order. Therefore, an early numerical evaluation by Kramer (1972) may be expected to provide valid results. Figure 2.9 shows comparisons between first- and second-order results for both the total charge-exchange cross section and the cross section differential in scattering angle, which reflects the dependence of the charge-exchange probability on impact parameter.

In the total cross section (Fig. 2.9left) you see that a major improvement is the step from the Brinkman-Kramers to the Jackson-Schiff result, while the second Born approximation provides a further, but only minor decrease. The differential cross section drops down to zero at some intermediate angle. This reflects a change in sign of the transition amplitude. According to Horsdal-Pedersen (1981) this dip is a general phenomenon related to the way how the nucleus-nucleus interaction is taken into account in the hamiltonian.

Calculations for other systems with $Z_1 = Z_2$ were performed by Belkić et al. (1987), and for $Z_1 \neq Z_2$ by Decker and Eichler (1989). Note here that the number of integrations invoked in (2.46) is prohibitively large for numerical evaluation in general. While it is tempting, as a first step, to carry out the summation over j, this is not straightforward since a simple closure relation

$$\sum_j \psi_j(\boldsymbol{r},t)\psi_j(\boldsymbol{r}',t) = \delta(\boldsymbol{r}-\boldsymbol{r}') \tag{2.76}$$

holds only for $t = t'$. Therefore, an approximation has frequently been used where the intermediate states are approximated by free-particle wave functions,

$$u_j(\boldsymbol{r},t) = \frac{1}{(2\pi)^{3/2}} \mathrm{e}^{\mathrm{i}[\boldsymbol{k}\cdot\boldsymbol{r}-(\hbar k^2/2m)t]}. \tag{2.77}$$

With this, the sum over j reduces to an integration over $\boldsymbol{k}$,

$$\sum_j \psi_j(\boldsymbol{r},t)\psi^*(\boldsymbol{r},t') = \frac{1}{(2\pi)^3} f(t,t') \int \mathrm{d}^3\boldsymbol{k}\, \mathrm{e}^{\mathrm{i}\boldsymbol{k}\cdot(\boldsymbol{r}-\boldsymbol{r}')} \mathrm{e}^{-\mathrm{i}(\hbar k^2/2m)(t-t')} \tag{2.78}$$

with

$$f(t,t') = \exp\left(\mathrm{i}\nu_1 \ln\frac{R-vt}{R-vt'}\right). \tag{2.79}$$

This integral can be evaluated in closed form (Problem 2.5), so that

$$\sum_j \psi_j(\boldsymbol{r},t)\psi^*(\boldsymbol{r},t') = \mathrm{e}^{-3\mathrm{i}\pi/4}\left(\frac{m}{2\pi\hbar(t-t')}\right)^{3/2} f(t,t') \exp\left[\mathrm{i}\frac{m(\boldsymbol{r}-\boldsymbol{r}')^2}{2\hbar(t-t')}\right] \tag{2.80}$$

2.4.5.2 Distorted-Wave Picture

Distorted-wave scattering theories are perturbation expansions in which part of the perturbation has been incorporated into the zero-order wave function. In other words, an interaction potential $\mathcal{V}_{\mathrm{DW}}(r,t)$ is adopted which allows for an analytic or at least accurate nonperturbational determination of zero-order wave functions. The subsequent perturbation expansion operates on the basis of an effective interaction $\mathcal{U}(r,t) = \mathcal{V}(r,t) - \mathcal{V}_{\mathrm{DW}}(r,t)$ which is weaker than the actual interaction $\mathcal{V}(r,t)$ and therefore leads to a more rapidly converging perturbation series.

Thus, perturbation theory as outlined in Sect. 2.4.3 is a distorted-wave theory with the special choice of $\mathcal{U}_{\mathrm{DW}}(r,t) = V_1(r) - V_1(R(t))$. We have seen that this rearrangement of the interaction implies the phase factor $\mathrm{e}^{-\mathrm{i}\alpha(t)/\hbar}$. However, in the literature on charge exchange these features do not always appear together: There are distorted-wave theories which do not incorporate a phase factor, or allow for a phase factor only in either the incoming or the outgoing wave.

The success of a distorted-wave theory hinges on a suitable model interaction which approximates the real interaction and, at the same time, allows to find appropriate wave functions in zero order, preferrably exact ones. Since deviations from free undisturbed motion are expected to be most pronounced at maximum interaction, distorted-wave potentials have typically a short range.

Calculations on charge exchange with DW models have been performed by many authors starting from Cheshire (1964). For analytical convenience, DW potentials frequently depend on the time variable only. A popular choice is

$$\mathcal{V}_{\mathrm{DW}}(t) = \int \mathrm{d}^3\boldsymbol{r}\; \psi_0^*(\boldsymbol{r},t)\, \mathcal{V}(\boldsymbol{r},t)\, \psi_0(\boldsymbol{r},t) \tag{2.81}$$

which, for a hydrogen-like target and an interaction of the form of (2.24), leads to

$$\mathcal{V}_{\mathrm{DW}}(t) = Z_1 e^2 \left(\frac{1}{R(t)} + \frac{1}{a}\right) \mathrm{e}^{-2R(t)/a}\,, \tag{2.82}$$

as you may find by solving Problem 2.6. Selected results will be shown below.

2.4.5.3 Eikonal Approximation

Consider the function

$$\psi_{\mathrm{eik}}(\boldsymbol{r},t) = \mathrm{e}^{-\mathrm{i}\mathcal{S}(\boldsymbol{r},t)/\hbar}\, \psi_0(\boldsymbol{r},t)\,, \tag{2.83}$$

where

$$\mathcal{S}(\boldsymbol{r},t) = \int^t \mathrm{d}t'\, \mathcal{V}(\boldsymbol{r},t) \tag{2.84}$$

and $\psi_0(\boldsymbol{r},t)$ is an eigenfunction to $\mathcal{H}_0$. $\psi_{\mathrm{eik}}(\boldsymbol{r},t)$ is not an exact solution to the Schrödinger equation, $[\mathcal{H}_0 + \mathcal{V}(\boldsymbol{r},t)]\psi(\boldsymbol{r},t) = \mathrm{i}\hbar\partial\psi(\boldsymbol{r},t)/\partial t$, but you may easily

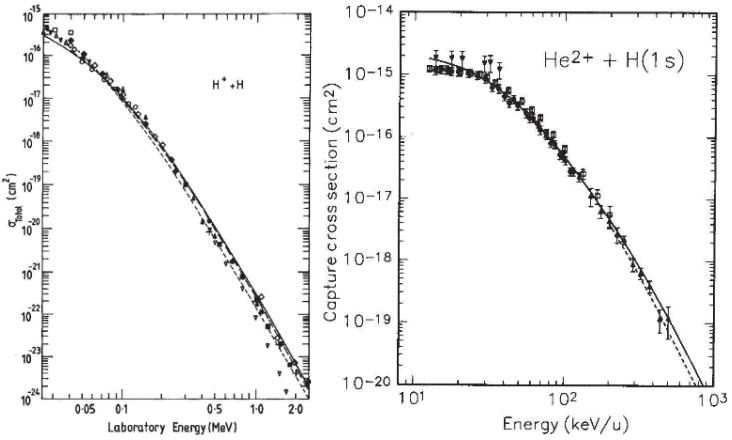

Fig. 2.10 Left: Total capture cross section for H^+-H. Solid line: B1B approximation (Belkić et al., 1987); dotted line: CDW approximation (Belkić et al., 1979); dashed line: Eikonal approximation (Dewangan and Eichler, 1994). Right: Same for He^{++}-H. Solid line: B1B approximation (Belkić et al., 1987); dotted line: CDW approximation (Belkić and Janev, 1973, Belkić et al., 1992). Experimental data refer to atomic hydrogen quoted by Dewangan and Eichler (1994). From Dewangan and Eichler (1994)

verify that

$$\mathrm{i}\hbar\frac{\partial\psi_{\mathrm{eik}}(\boldsymbol{r},t)}{\partial t} = [\epsilon_0 + \mathcal{V}(\boldsymbol{r},t)]\,\psi_{\mathrm{eik}}(\boldsymbol{r},t)\,. \tag{2.85}$$

Therefore, $\psi_{\mathrm{eik}}(\boldsymbol{r},t)$ will normally be a better approximation to the exact wave function than the zero-order approximation $\psi_0(\boldsymbol{r},t)$, where $\mathcal{V}(\boldsymbol{r},t)$ would be missing on the right-hand side of (2.85).

The quantity $\mathcal{S}(t)$ as defined by (2.84) is called the eikonal. A similar quantity in optics is called the optical path. The eikonal approximation (2.83) is a standard scheme in quantum mechanics (Schiff, 1981), which was introduced into scattering theory by Molière (1947).

In the context of (2.24), the eikonal reads

$$\begin{aligned}\mathcal{S}(\boldsymbol{r},t) &= \int^t \mathrm{d}t'\left[V_1(|\boldsymbol{r}-\boldsymbol{R}(t)|) - V_1\left(R(t)\right)\right] \\ &= \frac{Z_1 e^2}{v}\ln\frac{v|\boldsymbol{r}-\boldsymbol{R}| + \boldsymbol{v}\cdot(\boldsymbol{r}-\boldsymbol{R})}{vR - \boldsymbol{v}\cdot\boldsymbol{R}}.\end{aligned} \tag{2.86}$$

You may note that $\mathcal{S} = 0$ for $t = \pm\infty$. This implies that the full phase factor $\exp(-i\alpha(t)/\hbar$ has to be added to the eikonal wave function in order that it satisfies the Coulomb boundary condition. This condition is fulfilled if $\psi_0(\boldsymbol{r},t)$ is taken in the boundary-corrected form, (2.30).

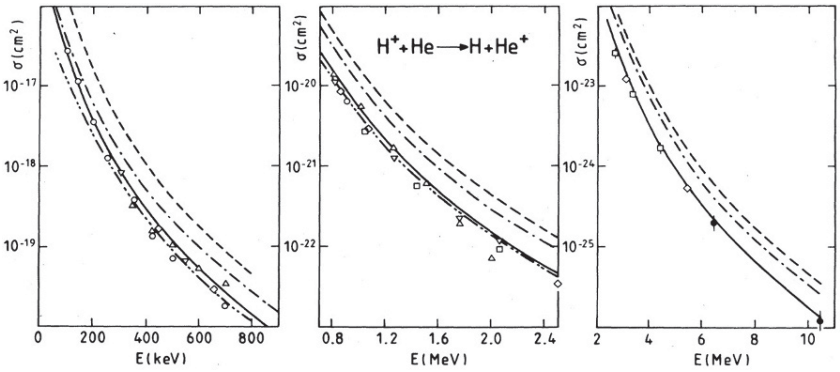

Fig. 2.11 Total capture cross sections for H^+-He for three energy intervals (left to right). Solid lines: B1B; dot-dashed lines: DWBA; dashed lines: OBK; double-dot-dashed lines: eikonal (Kobayashi et al., 1985). Experimental data quoted by Toshima et al. (1987). From Toshima et al. (1987)

2.4.5.4 Comparison with Experiment

The unperturbed wave function ψ_0, the CDW wave function ψ_{CDW} or the eikonal wave function ψ_{eik} can all serve as first-order approximations in a perturbation theory of charge exchange. Either approximation can be improved by going to the next order or by applying other approaches such as variational procedures.

Figure 2.10 shows results for protons in hydrogen. Calculations refer to atomic hydrogen as a target. Five sets of experimental data were likewise found with atomic hydrogen, while the remaining six data sets refer to molecular hydrogen. The agreement with experimental results appears very good, and differences between three theoretical results are comparable with the scatter of experimental data. Note that the cross section varies over almost nine orders of magnitude for an energy variation over only two orders of magnitude.

Figure 2.11 shows comparisons between several calculational schemes and measurements for H^+-He. It appears that the best agreement with experiment is achieved with the B1B and the eikonal method. However, calculations refer to $1s - 1s$ processes only, and the calculated cross sections were multiplied by a constant factor of 1.2 to account for the fact that measured cross sections do not differentiate between final states.

Figure 2.12 shows the measured differential cross section for charge exchange in H^+-He by Fischer et al. (2006) which was already shown in Fig. 2.3, but now compared with two theoretical results. Although the Thomas peak is clearly identified in both measurement and theory, quantitative agreement with experimental data does not appear better than about a factor of two. It is important here to note the angular scale: Considering the necessary angular resolution, it is a remarkable achievement by the experimentalists (Horsdal-Pedersen et al., 1983, Fischer et al., 2006) that the peak has been identified at all.

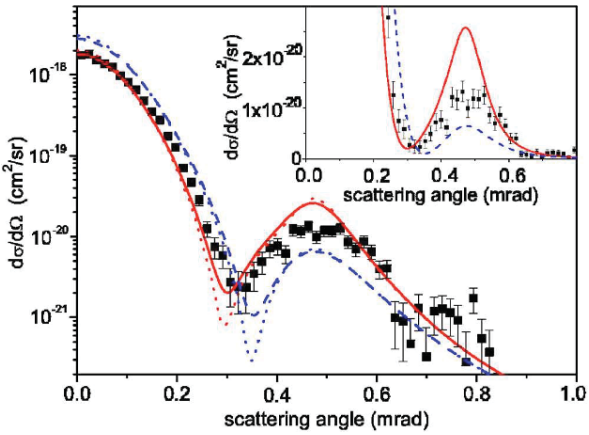

Fig. 2.12 Differential cross section for single-electron capture in 7.5 MeV H^+-He collision. Solid symbols: Measurements of Fischer et al. (2006). Solid line: CDW calculation (Abufager et al., 2005); dashed line: multiple-scattering (Faddeev) calculation (Adivi and Bolorizadeh, 2004). Theoretical calculations convoluted with the experimental resolution of the apparatus. Dotted lines: Theory before convolution. From Fischer et al. (2006)

2.5 Multiple-Electron Systems

2.5.1 Classical Models

A number of models for electron capture in a single event have been developed on the basis of classical collision theory. It is instructive to confront these models with quantal estimates to be discussed in the following section.

2.5.1.1 Bell Model

The estimate of Bell (1953) addressed electron capture from light gas atoms by fission fragments with a high projectile charge $q_1 e$. Even in a distant interaction, the force exerted by the projectile on a target electron can exceed its binding force. From the instant when this happens, the electron is considered only to interact with the projectile, and the effect of the target is ignored. The electron is considered as captured if its speed in the rest frame of the projectile is below the escape velocity.

Quantitative estimates on the basis of this model involve standard relations of classical Kepler motion. Trends of the capture cross sections were mentioned by Bell, but quantitative conclusions were only reported on equilibrium charges, which also invoke a model for electron loss.

Extensive calculations on the basis of a modified Bell model were performed by Gluckstern (1955).

2.5.1.2 Bohr-Lindhard Model

The model of Bohr and Lindhard (1954) likewise addresses capture and loss by fission fragments. Similar to Bell, they introduce a critical distance r_0 at which the Coulomb force due to the projectile balances the centrifugal force of the electron in its Kepler motion around the target nucleus. While the projectile approaches the target even further, the electron is assumed to gradually adjust its velocity toward the projectile speed, so that at some time its energy in the rest frame (kinetic plus potential) becomes zero. If this happens while the distance between the two nuclei is still less than r_0, the electron is considered as captured, so that the capture cross section is $\sigma_c = \pi r_0^2$.

On the basis of a simple atomic model, Bohr and Lindhard (1954) find

$$\sigma_c = \pi a_0^2 q_1^2 Z_2^{1/3} \left(\frac{v_0}{v}\right)^3 . \tag{2.87}$$

While this formula differs from Bohr's earlier expression, (2.9), you may recall that (2.87) is geared toward fission fragments, while (2.9) was developed with application to alpha particles in mind.

Bohr and Lindhard also note that the considered process favours electrons moving at a speed close to $v/2$, where only a minor adjustment in velocity is required for the electron to bind to the projectile, cf. Fig. 2.4 above. This condition may be difficult to fulfill for very light target atoms, with the consequence of electron capture becoming a rare process. By relaxing the criterion for capture, an alternative expression was found, valid specifically for weakly-bound target electrons, where

$$\sigma_c = \pi a_0^2 q_1^2 \left(\frac{v_0}{v}\right)^2 \frac{q_2^2}{n'^3} . \tag{2.88}$$

Here $q_2 e$ represents a screened charge of the target nucleus and n' an effective quantum number.

Knudsen et al. (1981b) applied the Bohr-Lindhard model in conjunction with a simple atomic model to establish an approximate scaling relationship for capture cross sections for a wide range of collision systems. Figure 2.13 shows a comparison of their formula with a large number of experimental data. While the scaling is by no means perfect, the formula may well provide a reliable order-of-magnitude estimate of a capture cross section in situations where experimental data are unavailable.

2.5.1.3 Straight Simulation

Computer simulation, i.e., straight numerical solution of the pertinent equations of motion has become increasingly successful with the development of powerful computers. In the context of charge exchange, pertinent equations of motion are Newton's second law as well as the Schrödinger and the Dirac equation.

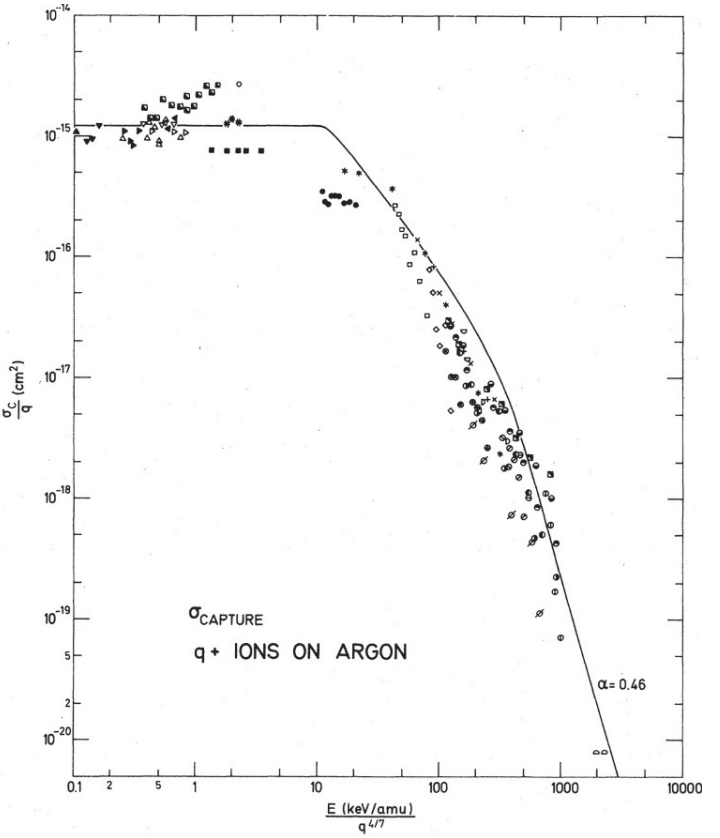

Fig. 2.13 Capture cross section for positive ions in argon. Experimental data for N, O, F, Ne, Ar, Br, Kr, I, Xe and W ions with charges q varying from 4 to 17 from a large number of sources quoted by Knudsen et al. (1981a) and compared with an empirical scaling relation. From Knudsen et al. (1981a)

We have seen that a classical description may well be appropriate if certain conditions are fulfilled. However, proper incorporation of the orbital motion of target and projectile electrons makes even the simplest collision systems untractable by conventional mathematical methods. This stimulated Abrines and Percival (1966a) to establish a straight numerical approach, which now goes under the label CTMC, or classical-trajectory Monte Carlo Calculation.

CTMC invokes three steps,

- the preparation of a statistical sample,
- simulating the dynamics of each configuration, and
- a statistical analysis of the outcome.

Quantum mechanics enters implicitly via input parameters such as binding energies and velocity distributions of the electrons. Obtaining accurate results requires good

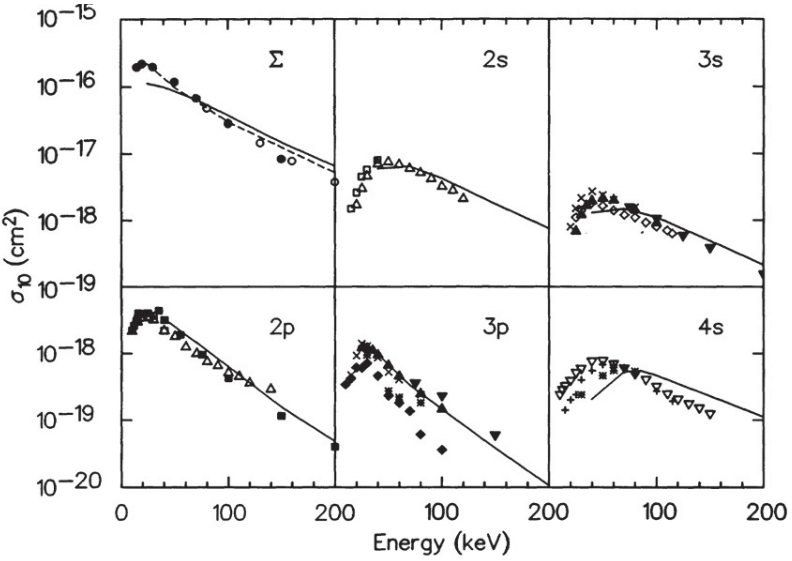

Fig. 2.14 State-separated cross sections for charge exchange in H^+-He collisions calculated by the CTMC method compared with experimental results. From Schultz et al. (1992)

statistics and, hence, extensive computation time. On the other hand, one and the same output obtained by this method can be used to extract a variety of quantities of physical interest, e.g., excitation and ionization cross sections.

Abrines and Percival (1966b) applied the scheme to charge exchange in H^+-H with good success. The range of applicability of the method has been greatly expanded by the work of Olson and Salop (1977), whose code has become a standard tool in atomic-collision theory, in particular when highly-charged ions and high-Z_2 targets are involved. Figure 2.14 shows an example.

Numerical solutions of the Schrödinger equation have become common in atomic-collision physics. Such calculations can be performed by the 'coupled-channel' method, where the wave function is expanded in terms of some basis such as (2.37), but instead of solving the resulting set of linear equations by perturbation expansion, a complete numerical solution is found by defining a subset of a finite number of states that are supposed to govern the process considered.

The number of states involved in charge-exchange and ionization processes increases with increasing projectile velocity. Therefore, the applicability of this method is limited by computational power to not too high projectile speeds. Differential cross sections are less CPU-intensive than total cross sections which may require reliable results for a wide range of impact parameters.

An example is the the END (Electron Nuclear Dynamics) code, which was designed with a view to the kinetics of chemical reactions (Deumens et al., 1994). In this code the nuclear motion is described by quantal wave packets of width zero. The adopted formalism is a quantal version of the Lagrange formalism known from

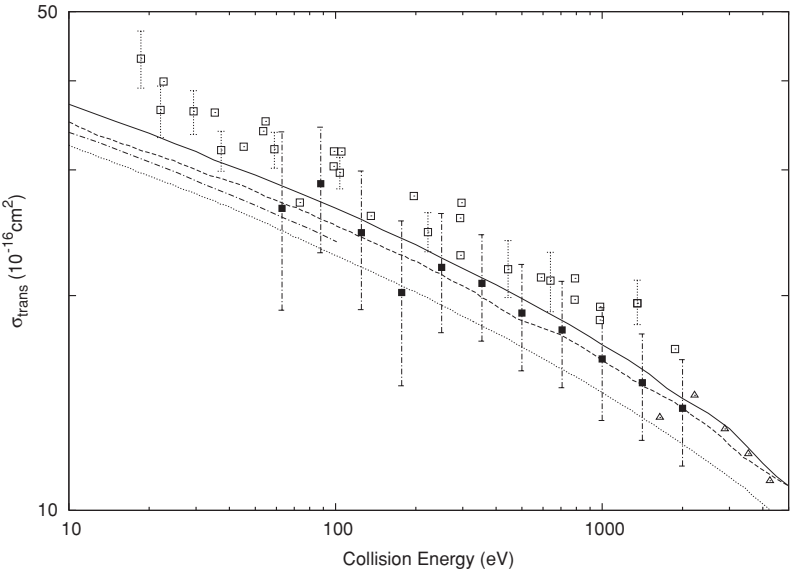

Fig. 2.15 Total capture cross section for H^+-H. Solid curve: END (Killian et al., 2004); Experimental data and other theoretical curves quoted by Killian et al. (2004). From Killian et al. (2004)

classical mechanics. The forward and backward coupling between electronic and nuclear motion is taken into account, as well as electron-electron interaction. In that sense, the code is suitable for application in systems containing many electrons, but the main limitations is available computational power. An example is shown in Fig. 2.15.

2.5.2 Data

An extensive compilation of calculated and measured capture cross sections may be found in three articles by Janev et al. (1983), Gallagher et al. (1983) and Janev and Gallagher (1983).

On the basis of empirical scaling relations found by Alonso and Gould (1982), Knudsen et al. (1981a), Ryufuku (1982) and Janev et al. (1980), Schlachter et al. (1983) proposed the empirical scaling relation

$$\sigma_c = \frac{\sqrt{q_1}}{Z_2^{1.8}} \frac{1.1 \times 10^{-8}}{\tilde{E}^{4.8}} \left(1 - \mathrm{e}^{-0.037\tilde{E}^{2.2}}\right) \left(1 - \mathrm{e}^{-2.44\times10^{-5}\tilde{E}^{2.6}}\right) , \qquad (2.89)$$

where

$$\tilde{E} = \frac{E}{Z_2^{1.25} q_1^{0.7}} , \qquad (2.90)$$

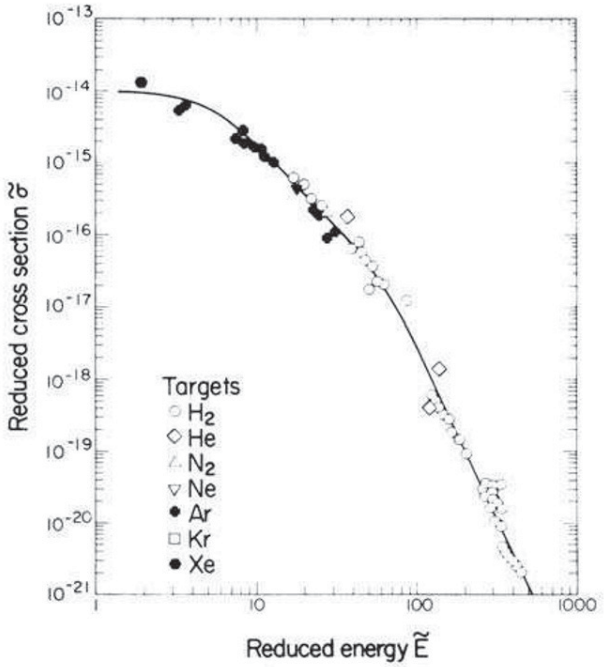

Fig. 2.16 Scaling of electron capture cross sections according to Schlachter et al. (1983). Solid line: (2.89). Points: Measured. From Schlachter et al. (1983)

with σ_c in cm^2 and E in keV/u. Here, the $\tilde{E}^{-4.8}$ dependence determines the high-energy behaviour for $\tilde{E} \gtrsim 100$. The second factor causes a bend-over in the interval $10 \lesssim \tilde{E} \lesssim 100$, and the last factor causes a further bend-over so that the function approaches a constant for $\tilde{E} < 10$. An example is shown in Fig. 2.16.

Comparisons with measurements on a number of systems were performed by Shevelko et al. (2010). Two examples, referring to measurements with Ge^{31+} on Ne (Stöhlker et al., 1992) and Xe^{18+} on N_2 (Olson et al., 2002), are shown in Fig. 2.17. The agreement achieved with (2.89) and theoretical estimates, CTMC and eikonal approximation (Stöhlker et al., 1992) as well as CDW and the CAPTURE code (Shevelko et al., 2004) illustrates the statement by Tolstikhina and Shevelko (2013) that 'getting an accuracy within a factor of 2 is a rather tedious task'.

2.6 Radiative Electron Capture ⋆

It has been mentioned in Sect. 2.2 that an ion may capture a free electron if the process is accompanied by the emission of a photon. This process, illustrated schemati-

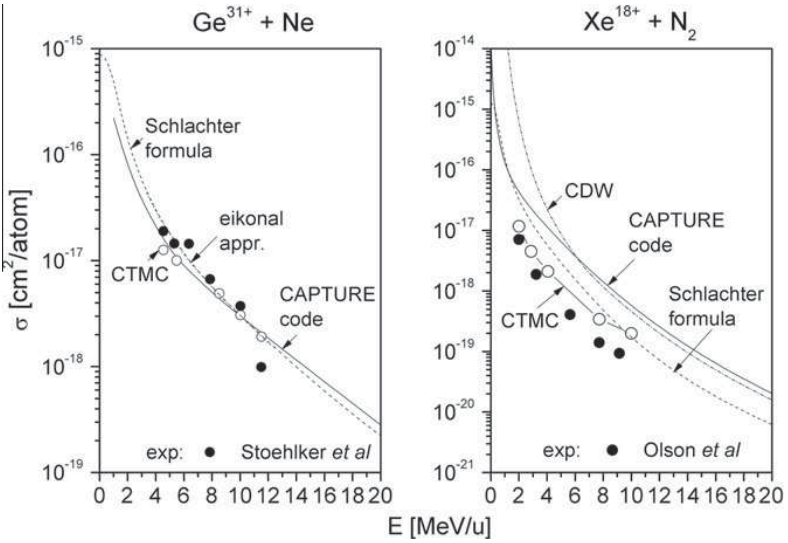

Fig. 2.17 Comparison of measured single-electron capture cross sections with semi-empirical formula and theoretical estimates. See text. From Shevelko et al. (2010)

cally in the left part of Fig. 2.18, is called *radiative recombination*. The right part of the figure indicates that radiative recombination is the inverse of the wellknown photoemission (or photoelectric emission) process. Radiative recombination can also take place with an electron that is initially bound to another atom or molecule. Then we talk about 'radiative electron capture'.

The existence of this effect was deduced by Raisbeck and Yiou (1971) from measurements of equilibrium charge states of high-energy (40–600 MeV) protons penetrating thin metal foils.

Subsequently, Schnopper et al. (1972) found X-ray emission in experiments with S, Cl and Br ions with energies up to 140 MeV. Ions in that energy range are highly charged, so that the emission of characteristic X-rays is greatly reduced. Measured continuous X-ray spectra were ascribed to radiative electron capture.

Kienle et al. (1973) made similar experiments with N, Ne and Ar beams at energies up to 288 MeV and, in addition to demonstrating convincing comparisons with theory, identified that also Bremsstrahlung was active.

From the experimental conditions specified here you may get an impression of radiative electron capture being a high-velocity phenomenon. Let us see how we can get at an estimate without diving too much into relativistic collision theory.

Fig. 2.18 Radiative recombination (left) and photoemission (right)

2.6.1 Detailed Balance

Figure 2.18 suggests a relation between photoemission and radiative recombination. One condition that must be common to both phenomena is energy conservation,

$$\hbar\omega = U + E_\mathrm{e}\,, \tag{2.91}$$

where $\hbar\omega$ is the photon energy, E_e the kinetic energy of the free electron and U the binding energy of the electron in the atom.

However, also the cross sections are related. To appreciate this, consider first an elastic collision between two particles 1 and 2. In Chap. 3, Vol. 1 we have considered the differential cross section both classically and quantally and have moved freely between the laboratory and the centre-of-mass frame of reference. We also made use of a reference frame in which the projectile was at rest. The differential cross section was expressed in various variables, but its magnitude was independent of the frame of reference, at least in the nonrelativistic limit. Indeed, in classical nonrelativistic collision theory the differential cross section is equal to an area $2\pi p\,dp$, the magnitude of which is the same, whether viewed from the laboratory, the projectile or any other reference frame.

The process shown in Fig. 2.18 is not an elastic collision, hence the above argument does not apply here. However, the *transition probability* must be independent of the arrow of the time, as long as energy conservation is fulfilled. This is called the *principle of detailed balance*. You may convince yourself of this by looking into Problem 2.7. In order to convert it into a relation between cross sections we employ the definition emerging from (2.1), Vol. 1, where the cross section for an event was found to be given by the ratio of the mean number of events per unit time and the incident current density.

Following Landau and Lifshitz (1960) we consider a reaction between two particles which results in a change of their identity, so that 1 and 2 represent the state of the system before and after the interaction. If the initial state is specified, the final state will represent a variety of configurations, such that the probability for transition to a given state j_2 is given by some function $P(j_1, j_2)$. In the reverse process, on the other hand, it is the state j_2 that is specified, while j_1 comprises a variety of configurations. The time reversal implied by the Schrödinger equation, on the other hand, specifies both the initial and the final state.

It is convenient to consider a finite normalization volume L^3 here, as has been done in Sect. 5.7.1, Vol. 1, so that a free particle is characterized by a wave function

$$\psi_{\boldsymbol{k}}(\boldsymbol{r}) = \frac{1}{L^{3/2}} \mathrm{e}^{\mathrm{i}\boldsymbol{k}\cdot\boldsymbol{r}} \tag{2.92}$$

with $\boldsymbol{k} = (\nu_x, \nu_y, \nu_z)2\pi/L$.

The total number of quantum states in an element $\mathrm{d}^3\boldsymbol{k}$ in momentum space (disregarding spin) is then given by

$$\left(\frac{L}{2\pi}\right)^3 \mathrm{d}^3\boldsymbol{k}\,. \tag{2.93}$$

We may then express the transition probability by a probability density w_{12},

$$P(j_1, j_2) \to w_{12} \left(\frac{L}{2\pi}\right)^3 \mathrm{d}^3\boldsymbol{k}_2\,. \tag{2.94}$$

where both the incident and the final configuration represent single quantum states. Hence the quantity w_{12} so defined must satisfy detailed balance,

$$w_{12} = w_{21}\,. \tag{2.95}$$

We may write the cross section $\mathrm{d}\sigma_{12}$ in the form

$$\mathrm{d}\sigma_{12} = \mathrm{d}K_{12}\delta(E_1 - E_2)\mathrm{d}E_2\,, \tag{2.96}$$

where the Dirac function represents energy conservation, cf. (2.91), while $\mathrm{d}K_{12}$ contains all other dependencies.

The transition probability is given by the product of the cross section, and the incident current density, so that

$$w_{12} = \left(\frac{2\pi}{L}\right)^3 v_1 N_1 \mathrm{d}K_{12}\delta(E_1 - E_2)\frac{\mathrm{d}E_2}{\mathrm{d}^3\boldsymbol{k}}\,, \tag{2.97}$$

where N_1 and v_1 represent the number of incident particles per volume and their speed, respectively.

The same relation holds for the inverse process with subscripts 1 and 2 interchanged. With this, (2.95) reduces to

$$v_1\,\mathrm{d}K_{12}\,\frac{\mathrm{d}E_2}{k_2^2\mathrm{d}k_2\mathrm{d}^2\Omega_2} = v_2\,\mathrm{d}K_{21}\,\frac{\mathrm{d}E_1}{k_1^2\mathrm{d}k_1\mathrm{d}^2\Omega_1}\,, \tag{2.98}$$

where we have set $N_1 = N_2 = 1/L^3$, i.e., one incident particle in either process.

Now, let state 1 represent a photon and 2 an electron, so that $\mathrm{d}K_{12}$ is the cross section for photoemission and $\mathrm{d}K_{21}$ the cross section for radiative recombination. Then,

$$E_1 = \hbar k_1 c; \quad v_1 = c \tag{2.99}$$

and

$$E_2 = \hbar^2 k_2^2/2m; \quad v_2 = \hbar k_2/m\,, \tag{2.100}$$

so that (2.98) reduces to

$$k_1^2 \frac{\mathrm{d}K_{12}}{\mathrm{d}^2\Omega_2} = k_2^2 \frac{\mathrm{d}K_{21}}{\mathrm{d}^2\Omega_1} \tag{2.101}$$

or

$$\frac{\mathrm{d}\sigma_{\mathrm{RR}}}{\mathrm{d}\Omega} = \left(\frac{\hbar\omega}{mvc}\right)^2 \frac{\mathrm{d}\sigma_{\mathrm{ph}}}{\mathrm{d}\Omega} \tag{2.102}$$

With this, the problem has been reduced to finding a cross section for photoemission, a classic topic from the early days of quantum theory.

2.6.2 Photoemission

In order to find the latter we have to go back to the problem of excitation of an atom by an electromagnetic wave which has been considered in Sect. A.5.2, Vol. 1. That treatment was based on the dipole approximation, i.e., long wavelength or low photon energy. This assumption does not necessarily apply when we want to consider radiative electron capture by swift ions. Here, the mismatch between the orbital speed and the ion speed is typically so large that photon energies will lie in the x ray or even gamma regime.

Quantal calculations of the cross section for photoemission were initiated by Wentzel (1926) and followed up by Sommerfeld and Schur (1930) and Stobbe (1930).

The interaction of an electron with an electromagnetic field can be described by a hamiltonian

$$H = \frac{1}{2m}\left(\boldsymbol{P} + \frac{e}{c}\boldsymbol{A}\right)^2 - e\Phi\,, \tag{2.103}$$

where $\boldsymbol{A}$ and Φ denote the vector and scalar potential, respectively[4] and $\boldsymbol{P}$ the momentum.

We may describe a monochromatic electromagnetic wave by

$$\boldsymbol{A} = \boldsymbol{A}_0 \cos(\boldsymbol{k}\cdot\boldsymbol{r} - \omega t); \qquad \boldsymbol{k}\cdot\boldsymbol{A}_0 = 0; \qquad \Phi = 0\,. \tag{2.104}$$

This is equivalent with an electric field

$$\boldsymbol{E} = \boldsymbol{E}_0 \sin(\boldsymbol{k}\cdot\boldsymbol{r} - \omega t) \tag{2.105}$$

for $\boldsymbol{A}_0 = c\boldsymbol{E}_0/\omega$. With this, the interaction of the wave with a Z-electron atom may be described by a hamiltonian

[4] As everywhere else in this monograph we operate in gaussian units here. For translation to SI units refer to Sect. A.1.1, Vol. 1 or to Jackson (1975).

$$\mathcal{H} = H + \mathcal{V}\,, \tag{2.106}$$

where H is the hamiltonian of the free atom and

$$\mathcal{V} = \frac{e}{mc} \sum_{\nu=1}^{Z} \boldsymbol{A}(\boldsymbol{r}_\nu, t) \cdot \boldsymbol{P}_\nu\,. \tag{2.107}$$

We have dropped the quadratic term in $\boldsymbol{A}$ since we are only going up to the first order in a perturbation expansion.

Assume the field to be switched on at $t = 0$ and to be switched off at $t = t_1$. Then, the transition amplitude from the initial state $|0\rangle$ to a state $|j\rangle$ is given by

$$c_j(t_1) = \frac{1}{\mathrm{i}\hbar} \int_0^{t_1} \mathrm{d}t\, \mathrm{e}^{\mathrm{i}\omega_{j0}t}\, \langle j|\mathcal{V}|0\rangle \tag{2.108}$$

according to (4.37), Vol. 1, or

$$c_j(t_1) = -\frac{e}{2\hbar mc} \left(\left\langle j \left| \sum_\nu \mathrm{e}^{\mathrm{i}\boldsymbol{k}\cdot\boldsymbol{r}_\nu} \boldsymbol{A}_0 \cdot \boldsymbol{P}_\nu \right| 0 \right\rangle \frac{\mathrm{e}^{\mathrm{i}(\omega_{j0}-\omega)t} - 1}{\omega_{j0} - \omega} + \left\langle j \left| \sum_\nu \mathrm{e}^{-\mathrm{i}\boldsymbol{k}\cdot\boldsymbol{r}_\nu} \boldsymbol{A}_0 \cdot \boldsymbol{P}_\nu \right| 0 \right\rangle \frac{\mathrm{e}^{\mathrm{i}(\omega_{j0}+\omega)t} - 1}{\omega_{j0} + \omega} \right). \tag{2.109}$$

Here,

$$\hbar\omega_{j0} = E_j - E_0 \tag{2.110}$$

represents the excitation energy. The denominator in the first term in the brackets of (2.109) indicates that this term is going to be large when the photon energy $\hbar\omega$ comes close to $\hbar\omega_{j0}$. By the same argument we may deduce that the second term, with $\omega + \omega_j$ in the denominator, is small by comparison in the present context and will be neglected.

The transition probability per unit time is then given by

$$w = \frac{1}{t_1} \sum_j |c_j(t_1)|^2 = \frac{e^2}{\hbar^2 m^2 c^2 t_1} \times \sum_j \left| \left\langle j \left| \sum_\nu \mathrm{e}^{\mathrm{i}\boldsymbol{k}\cdot\boldsymbol{r}_\nu} \boldsymbol{A}_0 \cdot \boldsymbol{P}_\nu \right| 0 \right\rangle \right|^2 \left(\frac{\sin \frac{(\omega_{j0}-\omega)t_1}{2}}{\omega_{j0} - \omega} \right)^2, \tag{2.111}$$

as long as $w \ll 1$, where the sum over j goes over all states that are compatible with energy conservation, $\omega_{j0} = \omega$.

Before evaluating the sum, let us consider the matrix element in (2.111). Since we deal with electrons ejected at fairly high energies we may approximate the final state as a free-electron state,

$$|j\rangle = \frac{1}{L^{3/2}} \mathrm{e}^{\mathrm{i}\boldsymbol{k}_j \cdot \boldsymbol{r}} \,. \tag{2.112}$$

Then, in an independent-particle model of the atom we may write

$$\left\langle j \left| \sum_\nu \mathrm{e}^{\mathrm{i}\boldsymbol{k}\cdot\boldsymbol{r}_\nu} \boldsymbol{A}_0 \cdot \boldsymbol{P}_\nu \right| 0 \right\rangle = \frac{1}{L^{3/2}} \sum_\nu \int \mathrm{d}^3\boldsymbol{r}\, \mathrm{e}^{-\mathrm{i}\boldsymbol{k}_j\cdot\boldsymbol{r}} \mathrm{e}^{\mathrm{i}\boldsymbol{k}\cdot\boldsymbol{r}} \boldsymbol{P} u_\nu(\boldsymbol{r}) \,, \tag{2.113}$$

where $\boldsymbol{P} = -\mathrm{i}\hbar\nabla$ and $u_\nu(\boldsymbol{r})$ is the wave function describing the νth initially occupied single-electron state. By partial integration this reduces to

$$\left\langle j \left| \sum_\nu \mathrm{e}^{\mathrm{i}\boldsymbol{k}\cdot\boldsymbol{r}_\nu} \boldsymbol{A}_0 \cdot \boldsymbol{P}_\nu \right| 0 \right\rangle = \frac{\hbar}{L^{3/2}} \sum_\nu \left(\boldsymbol{A}_0 \cdot \boldsymbol{k}_j\right) \int \mathrm{d}^3\boldsymbol{r}\, \mathrm{e}^{\mathrm{i}(\boldsymbol{k}-\boldsymbol{k}_j)\cdot\boldsymbol{r}} u_\nu(\boldsymbol{r}) \,, \tag{2.114}$$

Going back to (2.111) we need to evaluate the sum over j. The condition $\omega_{j0} = \omega$ implies that only states in a thin shell with radius $\sqrt{2m(\hbar\omega - U)}$ in $\boldsymbol{k}$-space can be excited. Following (2.93) we may introduce a density of states $\varrho(E)$ in energy space by means of the relation

$$\varrho(E_j)\mathrm{d}E_j = \left(\frac{L}{2\pi}\right)^3 \int \mathrm{d}^3\boldsymbol{k} \,, \tag{2.115}$$

where the integration goes over all states with a specified energy. The sum over j is the replaced by an integration over E_j, which is conveniently performed by making the replacement

$$x = (\omega_{j0} - \omega)t_1/2 \tag{2.116}$$

and yields

$$w_{12} = \frac{e^2 k_j \mathrm{d}^2\Omega_j}{(4\pi)^2\hbar m c^2} \left(\boldsymbol{A}_0 \cdot \boldsymbol{k}_j\right)^2 \left| \sum_\nu \int \mathrm{d}^3\boldsymbol{r}\, \mathrm{e}^{\mathrm{i}(\boldsymbol{k}-\boldsymbol{k}_j)\cdot\boldsymbol{r}} u_\nu(\boldsymbol{r}) \right|^2 . \tag{2.117}$$

With a photon current density

$$\frac{cE_0^2}{8\pi\hbar\omega} = \frac{\omega A_0^2}{8\pi\hbar c} \tag{2.118}$$

we then find the differential cross section for photoemission

$$\mathrm{d}\sigma = \frac{e^2 k_j k_{jz}^2}{2\pi m c\omega} \mathrm{d}^2\Omega_j \left| \int \mathrm{d}^3\boldsymbol{r}\, \mathrm{e}^{\mathrm{i}(k_x - \boldsymbol{k}_j\cdot\boldsymbol{r})} u_\nu(\boldsymbol{r}) \right|^2 , \tag{2.119}$$

where the x-axis denotes the direction of propagation and the z-axis the polarization of the incident wave. This result, as well as the essence of the derivation, follows Schiff (1981).

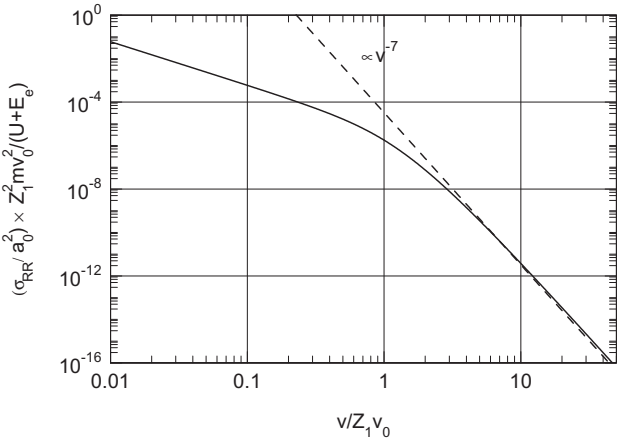

Fig. 2.19 Cross section σ_{RR} for radiative recombination according to the Stobbe formula (2.122)

2.6.3 Examples

For capture into the K shell, Stobbe (1930) finds the total cross section for radiative recombination, in the notation of Eichler and Meyerhof (1995),

$$\sigma_{\mathrm{ph}} = \frac{2^8\pi^2}{3}\frac{e^2}{mc\omega}\left(\frac{\nu^2}{1+\nu^2}\right)^3 \frac{\exp\left(-4\nu\arctan(1/\nu)\right)}{1-\exp(-2\pi\nu)}, \tag{2.120}$$

where ν is the Sommerfeld parameter

$$\nu = \frac{Z_1 e^2}{\hbar v}. \tag{2.121}$$

With this, and (2.102), the cross section for radiative recombination reads, in the nonrelativistic limit,

$$\sigma_{\mathrm{RR}} = \frac{2^8\pi^2}{3}\frac{\hbar\omega}{mv^2}a_0^2\alpha^3\left(\frac{\nu^2}{1+\nu^2}\right)^3 \frac{\exp\left(-4\nu\arctan(1/\nu)\right)}{1-\exp(-2\pi\nu)}, \tag{2.122}$$

where $\alpha = 1/137$ is the fine structure constant.

Figure 2.19 shows a universal plot of (2.122). It is seen that, due to the factor α^3, the absolute value of the capture cross section is small when taken in atomic units. However, with increasing projectile speed a $\propto v^{-7}$ dependence is approached which is much slower than that for nonradiative capture, going as $\propto v^{-11}$ or $\propto v^{-12}$.

An extensive discussion of the relativistic case has been given by Eichler and Meyerhof (1995), based on pioneering work by Sauter (1931a,b).

While (2.119) together with (2.98) shows essential features of radiative electron capture, such as the dependence on the frequency ω of the emitted X-ray as well as

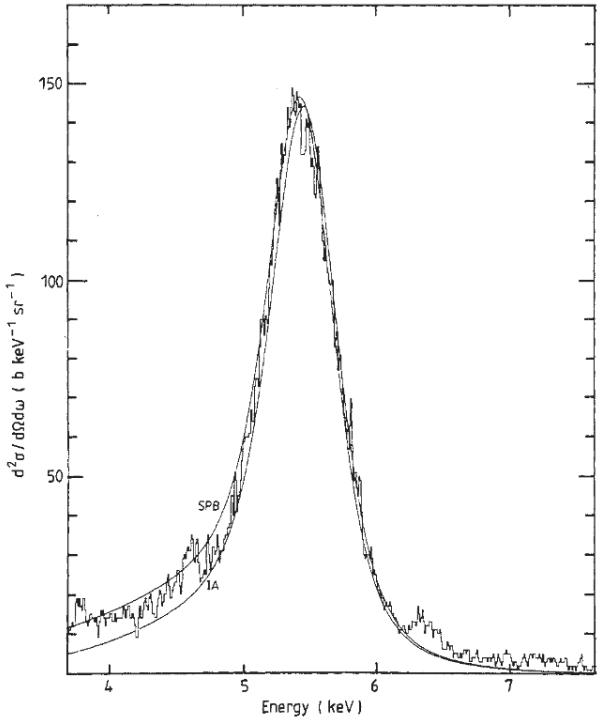

Fig. 2.20 Calculated and measured differential cross section for radiative electron capture to 125 MeV S^{16+} in carbon. Smooth curves represent strong-potential Born approximation (SPB) and impulse approximation (IA). From Jakubassa-Amundsen et al. (1984)

the order of magnitude of the effect, detailed theory is more complex (Kleber and Jakubassa, 1975, Eichler and Stöhlker, 2007).

Figure 2.20 shows an example of capture from carbon into the K shell of a fully-stripped sulphur ion. You may note first that the triply-differential cross section (solid angle and X-ray energy) is of the order of 100 b = 10^{-22} cm^2. The peak located between $\hbar\omega \simeq 5$ and 6 is made up primarily by the kinetic energy of a target electron in the rest frame of the ion, i.e., $mv^2/2$=2.1 keV and the K shell binding energy of 3.5 keV.

2.7 Electron Loss

From a theoretical point of view, electron loss is an ionization process seen from a reference frame moving with the projectile. For passage through a gaseous medium, the particle at rest in the moving reference frame is charged, while the one in motion

is neutral. For passage through a conducting medium it may be necessary also to consider ionization by free target electrons.

Both Volume 1 and the present volume in this monograph address primarily the first and the second moment over the energy-loss spectrum. The ionization cross section is related to the zero'th moment and, as such, is more sensitive to the behaviour near threshold. Since ionization phenomena are central to the topic of radiation effects, the treatment of ionization cross sections and ionization thresholds will be reserved to Volume 3. Therefore, the treatment of loss cross sections presented here is rather superficial.

2.7.1 Single and Multiple Loss

A look at stopping cross sections for heavy ions will tell you that ionization cross sections can be quite large, so that the probability for single, double and higher ionizations may become significant. This implies that we have to distinguish between single and multiple loss events.

Consider, for simplicity, ionization of a given shell containing n electrons in an atom at rest. In an independent-particle model, let $Q(\boldsymbol{p})$ be the probability per electron to be liberated after passage of a projectile at a vectorial impact parameter $\boldsymbol{p}$. Then, the probability for emission of exactly one electron is

$$P_1(\boldsymbol{p}) = nQ(\boldsymbol{p})\,[1 - Q(\boldsymbol{p})]^{n-1} \ . \tag{2.123}$$

Similarly, the probability for emission of two electrons is given by

$$P_2(w\,\boldsymbol{p}) = \frac{n(n-1)}{2}\,[Q(\boldsymbol{p})]^2\,[1 - Q(\boldsymbol{p})]^{n-2} \ . \tag{2.124}$$

In other words, the cross section for loss of ν electrons is given by

$$\sigma_\nu = \binom{n}{\nu} \int \mathrm{d}^2\boldsymbol{p}\ [Q(\boldsymbol{p})]^\nu\,[1 - Q(\boldsymbol{p})]^{n-\nu} \ . \tag{2.125}$$

For not too large values of $Q(\boldsymbol{p})$ we may approximate the cross section for single ionization by

$$\sigma_1 \simeq n \int \mathrm{d}^2\boldsymbol{p}\ Q(\boldsymbol{p}) - n(n-1) \int \mathrm{d}^2\boldsymbol{p}\ [Q(\boldsymbol{p})]^2 \tag{2.126}$$

and the cross section for double ionization by

$$\sigma_2 \simeq \frac{n(n-1)}{2} \int \mathrm{d}^2\boldsymbol{p}\ [Q(\boldsymbol{p})]^2 \ , \tag{2.127}$$

so that

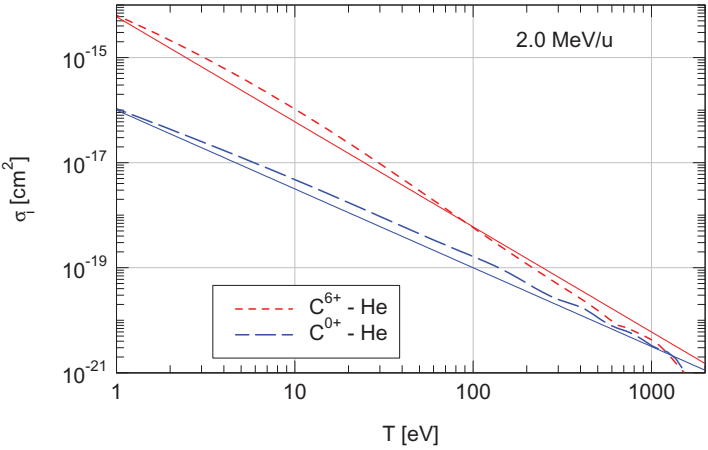

Fig. 2.21 Differential energy loss cross section for C-He collision according to PASS code (Weng et al., 2006) (dashed lines). Energy transferred to He atom. Neutral and fully-stripped carbon projectile. Solid lines: $\propto T^{-3/2}$ and $\propto T^{-2}$, respectively

$$\sigma_1 \simeq \sigma_I - 2\sigma_2\,, \tag{2.128}$$

where

$$\sigma_I = n \int \mathrm{d}^2\boldsymbol{p}\; Q(\boldsymbol{p}) \tag{2.129}$$

is the total ionization cross section.

These considerations can be formulated such as to invoke electrons from different shells (McGuire and Weaver, 1977). Rigourous definitions would have to involve transition amplitudes between many-body wave functions.

2.7.2 Theoretical Schemes

In principle, any theoretical scheme to treat ionization processes should be applicable to treat electron loss. This also includes theoretical schemes designed for stopping, such as the Bethe theory, binary theory or CasP.

Since ionization cross sections are determined primarily by energy transfers close to threshold, soft collisions provide the dominating contribution at least at high projectile speeds. In the present case, where the 'projectile' is a neutral atom, the screening of the Coulomb interaction implies that this dominance is weakened.

Figure 2.21 shows a comparison between differential energy-loss cross sections for neutral and fully-stripped carbon ions on helium, calculated by a version of the PASS code that generates differential energy-loss cross sections (Weng et al., 2006). This graph includes shell and Barkas-Andersen corrections. While the spectrum for fully-stripped C ions shows only a minor deviation from the T^{-2}-dependence for

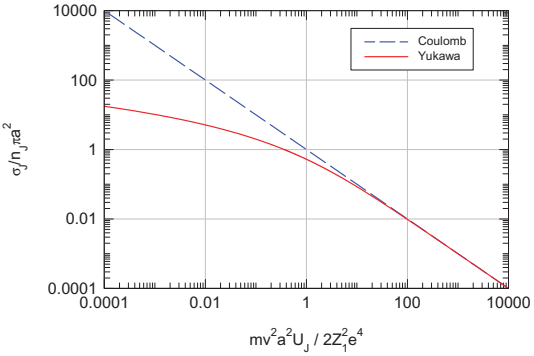

Fig. 2.22 Simple estimate of single-loss cross section σ_J. See text

free-Coulomb scattering, the spectrum for neutral carbon is very close to a $T^{-3/2}$ dependence.

The standard scheme for calculating ionization cross sections is the Born approximation (Inokuti, 1971). This scheme involves quite complex calculations, once the upper integration limit becomes essential.

It is useful here to recall the scaling properties of corrections to the straight Bethe theory of stopping:

- The shell correction is characterized by $\langle v_e^2 \rangle / v^2 \propto Z_2^{4/3} v_0^2 / v^2$,
- The Barkas-Andersen correction is characterized by the inverse of the parameter entering the Bohr stopping formula, $Z_1 e^2 \omega / m v^3 \propto Z_1 Z_2 v_0^3 / v^3$,
- The screening correction is characterized by $v_{TF}^2 / v^2 \propto Z_1^{4/3} v_0^2 / v^2$.

Thus, calculations on the basis of the Born approximation will be appropriate for light ions, provided that shell corrections are taken into account. Conversely, whatever scheme is employed for heavy ions, projectile screening need to be considered. The role to be assigned to the Barkas-Andersen correction depends on the desired accuracy.

Like the Born approximation, the classical-trajectory-Monte-Carlo (CTMC) simulation method (Olson et al., 1989) differentiates between single and multiple ionization events.

In the regime of dominating single ionization, classical binary scattering is most convenient. Assume the interaction between a neutral atom and a projectile electron to be given by

$$V(r) = \frac{-Z_1 e^2}{r} \phi(r/a)\,, \tag{2.130}$$

with a given screening function and radius, ϕ and a, respectively. Then, from (3.76) and (3.8), Vol. 1 you will be able to derive a relation for the energy loss

$$T = T(v, p) \tag{2.131}$$

to a projectile electron, where v is the projectile speed and p the impact parameter between a projectile electron and a target nucleus. The loss cross section for a given shell J is then given by

$$\sigma_J = n_J \pi p_J^2 \,, \tag{2.132}$$

where p_J is defined by

$$T(v, p_J) = U_J \,, \tag{2.133}$$

U_J being the ionization energy of the Jth shell. Such a calculation includes screening but ignores Barkas-Andersen and shell corrections.

Figure 2.22 shows an example for $\phi(r/a) = \exp(-r/a)$, where the scattering integral can be evaluated analytically (cf. Problem 2.8). Also included is the estimate for straight Coulomb interaction,

$$\sigma_J = \frac{2\pi n_J Z_1^2 e^4}{m v^2 U_J} \,. \tag{2.134}$$

Even though the accuracy of the Yukawa prediction deteriorates at low energies, you will note that the difference to the Coulomb cross section becomes substantial.

2.7.3 Data

Numerous available experimental data for both capture and loss cross sections may be found in compilations. Lo and Fite (1969) offer data for both gaseous and metallic ions in gas targets over en energy range covering the keV and lower MeV region. Dehmel et al. (1973) cover a similar energy range with many more data and include a bibliography ordered by ion-target combination. Tables by Tawara et al. (1985) and Janev et al. (1988), focusing on nuclear fusion, offer extensive data for charge exchange in atomic and molecular hydrogen as well as helium. Dmitriev et al. (2010) provide a summary of their own data, taken over half a century and covering a broad spectrum of ion-target combinations in the keV/u energy range.

Calculated capture and loss cross sections at higher energies can be extracted from output of the ETACHA code (Rozet et al., 1996) for $Z_1 \leq 36$. The LOSS code by Shevelko et al. (2001) delivers calculated electron loss cross sections for heavier ions at high energies.

2.8 Discussion and Outlook

Although the process of electron capture in atomic collisions was studied originally in connection with particle penetration, the subject has developed its own dynamics both from an experimental and a theoretical point of view. If you find that this chapter overemphasizes charge exchange in simple hydrogen-like collision systems,

you are unquestionably right, when comparing with monographs on related subjects such as Kumakhov and Komarov (1981) or Nastasi et al. (1996). On the other hand, this is only a rudimentary account of the effort spent in the field and reported by Bransden and McDowell (1992) or Dewangan and Eichler (1994).

Just as in other areas of ion-beam physics, there is a striking contrast between the degree of sophistication of both theory and experiment on the one hand, and the degree of agreement between theoretical predictions and experimental results on the other. Clearly there is space for improvement.

To the extent that charge exchange can be characterized by cross sections, the statistical theory aiming at equilibrium charges, fluctuations and approach to equilibrium can be developed without reference to specific ion-target combinations. This is the topic of the following chapter.

Problems

2.1. Show that (2.34) satisfies the Schrödinger equation

$$\mathcal{H}_1 \chi_\ell(\boldsymbol{r},t) = i\hbar \frac{\partial \chi_\ell(\boldsymbol{r},t)}{\partial t} \tag{2.135}$$

and demonstrate that the electron density is centered around the projectile position $\boldsymbol{R}(t)$.

2.2. Go through the derivation of (2.41) from (2.38). You need to write down the Schrödinger equation for the two pertinent hamiltonians. You will also need the relation

$$\int d^3\boldsymbol{r}\ \psi_1^*(\boldsymbol{r}) \boldsymbol{O} \psi_2(\boldsymbol{r}) = \int d^3\boldsymbol{r}\ [\boldsymbol{O}\psi_1(\boldsymbol{r})]^* \psi_2(\boldsymbol{r}) \tag{2.136}$$

for hermitian operators (Schiff, 1981).

2.3. Derive (2.63) from (2.61) for the H^+-H system using (2.62).

2.4. Find the velocity distribution $f(v_e)$ for the wave function (2.62) and determine the probability $P(v/2) = \int_{v/2}^{\infty} f(v_e) 4\pi v_e^2 dv_e$ for an electron to have a velocity $v_e > v/2$.

2.5. Derive (2.80) from (2.78) and demonstrate that (2.80) approaches a Dirac function $\delta(\boldsymbol{r} - \boldsymbol{r}')$ for $t \to t'$. [Hint: Show first that the integral over $\boldsymbol{r}'$ yields $f(t,t')$ for arbitrary t and t'. Then study the behaviour of the function for $t \to t'$].

2.6. Derive (2.82)

2.7. Demonstrate that, for an arbitrary collision event, the transition probability P_{12} from a state 1 to a state 2 of the particles involved, is identical with the probability for the inverse process P_{21}. Hint: Write $\psi_2 = S\psi_1$ and look at the properties of the operator S. If needed, consult Landau and Lifshitz (1960).

2.8. Try to reproduce Fig. 2.22 from the information given in the text.

References

Aaron R., Amado R.D. and Lee B.W. (1961): Divergence of the Green's function series for rearrangement collisions. Phys Rev **121**, 319–323

Abrines R. and Percival I.C. (1966a): Classical theory of charge transfer and ionization of hydrogen by protons. Proc Phys Soc **88**, 861–872

Abrines R. and Percival I.C. (1966b): A generalized correspondence principle and proton-hydrogen collisions. Proc Phys Soc **88**, 873–883

Abufager P.N., Fainstein P.D., Martinez A.E. and Rivarola R.D. (2005): Single electron capture differential cross section in He^+ + He collisions at intermediate and high collision energies. J Phys B **38**, 11–22

Adivi E.G. and Bolorizadeh M.A. (2004): Faddeev treatment of single-electron capture by protons in collision with many-electron atoms. J Phys B **37**, 3321–3338

Allison S.K. (1958): Experimental results on charge-changing collisions of hydrogen and helium atoms and ions at kinetic energies above 0.2 keV. Rev Mod Phys **30**, 1137–1168

Alonso J. and Gould H. (1982): Charge-changing cross-sections for Pb and Xe ions at velocities up to 4 x 109 cm/sec. Phys Rev A **26**, 1134–1137

Bates D.R. (1958): Electron capture in fast collisions. Proc Roy Soc A **247**, 294–301

Bates D.R. and Dalgarno A. (1952): Electron capture I: Resonance capture from hydrogen atoms by fast protons. Proc Phys Soc **A65**, 919–925

Belkić D., Gayet R. and Salin A. (1979): Electron-capture in high-energy ion-atom collisions. Phys Rep **56**, 279–369

Belkić D., Gayet R. and Salin A. (1992): Cross-sections for electron-capture from atomic-hydrogen by fully stripped ions. At Data Nucl Data Tab **56**, 59–150

Belkić D. and Janev R.K. (1973): Electron capture from atomic hydrogen and helium atoms by fast alpha particles. J Phys B **6**, 1020–1027

Belkić D., Saini S. and Taylor H.S. (1987): Critical test of first-order theories for electron transfer in collisions between multicharged ions and hydrogen: The boundary condition problem. Phys Rev A **36**, 1601–1617

Bell G.I. (1953): The capture and loss of electrons by fission fragments. Phys Rev **90**, 548–557

Betz H.D. (1972): Charge states and charge-changing cross sections of fast heavy ions penetrating through gaseous and solid media. Rev Mod Phys **44**, 465–539

Bohr N. (1940): Scattering and stopping of fission fragments. Phys Rev **58**, 654–655

Bohr N. (1941): Velocity-range relation for fission fragments. Phys Rev **59**, 270–275

Bohr N. (1948): The penetration of atomic particles through matter. Mat Fys Medd Dan Vid Selsk **18 no. 8**, 1–144

Bohr N. and Lindhard J. (1954): Electron capture and loss by heavy ions penetrating through matter. Mat Fys Medd Dan Vid Selsk **28 no. 7**, 1–31

Bransden B.H. and McDowell M.R.C. (1992): *Charge exchange and the theory of ion-atom collisions*. Clarendon Press, Oxford

Briggs J.S. (1977): Impact-parameter formulation of the impulse approximation for charge exchange. J Phys B **10**, 3075–3089

Brinkman H.C. and Kramers H.A. (1930): Zur Theorie der Einfangung von Elektronen durch Alpha-Teilchen. Proc Roy Acad Amsterdam **33**, 973–984

Cheshire I.M. (1964): Continuum distorted wave approximation; resonant charge transfer by fast protons in atomic hydrogen. Proc Phys Soc **84**, 89–98

Crothers D.F.S. and Holt A.R. (1966): The first Born approximation for collisions between heavy particles. Proc Phys Soc **88**, 75–81

Decker F. and Eichler J. (1989): Exact second-order Born calculations for charge exchange with Coulomb boundary conditions. J Phys B **22**, L95–L100

Dehmel R.C., Chau H.K. and Fleischmann H.H. (1973): Experimental stripping cross sections for atoms and ions in gases 1950-1970. Atomic Data **5**, 231–289

Dettmann K. (1971): Wave packet theory of Coulomb scattering. Z Physik **244**, 86

Deumens E., Diz A., Longo R. and Öhrn Y. (1994): Time-dependent theoretical treatments of the dynamics of electrons and nuclei in molecular systems. Rev Mod Phys **66**, 917–983

Dewangan D.P. and Eichler J. (1986): A first-order Born approximation for charge exchange with Coulomb boundary conditions. J Phys B **19**, 2939–2944

Dewangan D.P. and Eichler J. (1994): Charge exchange in energetic ion-atom collisions. Phys Rep **247**, 59–219

Dmitriev I.S., Teplova Y.A., Belkova Y.A., Novikov N.V. and Fainberg Y.A. (2010): Experimental electron loss and capture cross sections in ion-atom collisions. Atomic Data Nucl Data Tab **96**, 85–121

Drisko R.M. (1955): The theories of positronium and of rearrangement collisions. Ph.D. thesis, Carnegie-Mellon University

Eichler J. (1987): Theory of relativistic charge exchange with Coulomb boundary conditions. Phys Rev A **35**, 3248–3255

Eichler J. and Meyerhof W.E. (1995): *Relativistic atomic collisions*. Academic Press, San Diego

Eichler J. and Stöhlker T. (2007): Radiative electron capture in relativistic ion-atom collisions and the photoelectric effect in hydrogen-like high-Z systems. Physics Rep **439**, 1–99

Fischer D., Støchkel K., Cederquist H., Zettergren H., Reinhed P., Schuch R., Källberg A., Simonsson A. and Schmidt H.T. (2006): Experimental separation of the Thomas charge-transfer process in high-velocity p-He collisions. Phys Rev A **73**, 052713

Flamm L. and Schumann R. (1916): Die Geschwindigkeitsabnahme der α-Strahlen in Materie. Ann Physik **50**, 655

Gallagher J.W., Bransden B.H. and Janev R.K. (1983): Evaluated theoretical cross section data for charge exchange of multiply charged ions with atoms. II. Hydrogen atom-partially stripped ion systems. J Phys Chem Ref Data **12**, 873–890

Gluckstern R.L. (1955): Electron capture and loss by ions in gases. Phys Rev **98**, 1817–1821

Halpern A.M. and Law J. (1975): Full first Born approximation for inner-shell pickup in heavy-ion collisions. Phys Rev A **12**, 1776–1780

Henderson G.H. (1923): Changes in the charge of an alpha-particle passing through matter. Proc Roy Soc A **102**, 496–U14

Horsdal-Pedersen E. (1981): On the two-state approximation for capture. J Phys B **14**, L249–L253

Horsdal-Pedersen E., Cocke C.L. and Stockli M. (1983): Experimental observation of the Thomas peak in high-velocity electron capture by protons from He. Phys Rev Lett **50**, 1910–1913

Horvat V., Watson R.L. and Parameswaran R. (1995): Spectra of l-x-rays from fast highly-charged xe ions traveling in solids. Phys Rev A **51**, 363–373

Inokuti M. (1971): Inelastic collisions of fast charged particles with atoms and molecules – the Bethe theory revisited. Rev Mod Phys **43**, 297–347

Jackson J.D. (1975): *Classical electrodynamics*. John Wiley & Sons, New York

Jackson J.D. and Schiff H. (1953): Electron capture by protons passing through hydrogen. Phys Rev **89**, 359–365

Jakubassa-Amundsen D.H., Höppler R. and Betz H.D. (1984): Radiative electron capture in fast ion-atom collisions. J Phys B **17**, 3943–3949

Janev R.K., Bransden B.H. and Gallagher J.W. (1983): Evaluated theoretical cross section data for charge exchange of multiply charged ions with atoms. I. Hydrogen atom-fully stripped ion systems. J Phys Chem Ref Data **12**, 829–872

Janev R.K. and Gallagher J.W. (1983): Evaluated theoretical cross section data for charge exchange of multiply charged ions with atoms. III. Nonhydrogenic target atoms. J Phys Chem Ref Data **13**, 1199–1249

Janev R.K., Phaneuf R.A. and Hunter H.T. (1988): Recommended cross sections for electron capture and ionization in collisions of C^{q+} and O^{q+} ions with H, He and H_2. Atomic Data Nucl Data Tab **40**, 249–281

Janev R.K., Presnyakov L.P. and Shevelko V.P. (1980): One-electron capture from the inner shells in atom-multicharged ion collisions. Phys Lett A **76**, 121–124

Keene J.P. (1949): Ionization and charge exchange by fast ions of hydrogen and helium. Phil Mag **40**, 369–385

Kienle P., Kleber M., Povh B., Diamond R.M. and Stephens F.S. (1973): Radiative capture and bremsstrahlung of bound electrons induced by heavy ions. Phys Rev Lett **31**, 1099–1102

Killian B.J., Cabrera-Trujillo R., Deumen E. and Öhrn Y. (2004): Resonant charge transfer between H^+ and H from 1 to 5000 eV. J Phys B **37**, 4733–4747

Kleber M. and Jakubassa D.H. (1975): Radiative electron capture in heavy-ion collisions. Nucl Phys A **252**, 152–162

Knudsen H., Haugen H.K. and Hvelplund P. (1981a): Single-electron-capture cross section for medium- and high-velocity, highly charged ions colliding with atoms. Phys Rev A **23**, 597–610

Knudsen H., Haugen H.K. and Hvelplund P. (1981b): Single-electron capture cross section ofr medium- and high-velocity, highly charged ions colliding with atoms. Phys Rev A **23**, 597–610

Knudson A.R., Burghalter P.G. and Nagel D.J. (1974): Vacancy configurations of argon projectile ions in solids. Phys Rev A **10**, 2118–2122

Kobayashi K., Toshima N. and Ishihara T. (1985): Eikonal approximation for proton-helium electron capture processes. Phys Rev A **32**, 1363–1368

Kramer P.J. (1972): Exact calculation of the second-order Born terms for proton-hydrogen electron-transfer collisions. Phys Rev A **6**, 2125–2130

Kumakhov M.A. and Komarov F.F. (1981): *Energy loss and ion ranges in solids*. Gordon and Breach, New York

Landau L.D. and Lifshitz E.M. (1960): *Quantum mechanics. Non-relativistic theory*, vol. 3 of *Course of theoretical physics*. Pergamon Press, Oxford

Lassen N.O. (1951a): Total charges of fission fragments as functions of the pressure in the stopping gas. Mat Fys Medd Dan Vid Selsk **26 no. 12**, 1–19

Lassen N.O. (1951b): The total charges of fission fragments in gaseous and solid stopping media. Mat Fys Medd Dan Vid Selsk **26 no. 5**, 1–28

Lo H.H. and Fite W.L. (1969): Electron-capture and loss cross sections for fast heavy particles passing through gases. Atomic Data **1**, 305–328

Macek J. and Taulbjerg K. (1981): Correction to Z_p/Z_t expansions for electron-capture. Phys Rev Lett **46**, 170–174

Macek J.H. and Shakeshaft R. (1980): Second Born approximation with the Coulomb Green's function: Electron capture from a hydrogenlike ion by a bare ion. Phys Rev A **22**, 1441–1446

McDowell M.R.C. and Coleman J.P. (1970): *Introduction to the theory of ion-atom collisions*. North Holland Publ. Co., Amsterdam

McGuire J.H. and Weaver L. (1977): Independent electron approximation for atomic scattering by heavy particles. Phys Rev A **16**, 41–47

Mittleman M.H. (1964): Relativistic effects in charge transfer. Proc Phys Soc **84**, 453–454

Moiseiwitsch B.L. (1980): Relativistic effects in atomic collisions theory. Adv At Mol Phys **16**, 281–318

Molière G. (1947): Theorie der Streuung schneller geladener Teilchen I. Einzelstreuung am abgeschirmten Coulomb-Feld. Z Naturforsch **2a**, 133–145

Nastasi M., Hirvonen J.K. and Mayer J.W. (1996): *Ion-solid interactions: Fundamentals and applications*. Cambridge University Press, Cambridge

Nikolaev V.S. (1965): Electron capture and loss by fast ions in atomic collisions. Usp Fiz Nauk **85**, 679 – 720. [Engl. Transl. Sov. Phys. Uspekhi 8, 269 - 294 (1965)]

Olson R., Ullrich J. and Schmidt-Boecking H. (1989): Multiple-ionization collision dynamics. Phys Rev A **39**, 5572

Olson R.E. and Salop A. (1977): Charge-transfer and impact-ionization cross sections for fully and partially stripped positive ions colliding with atomic hydrogen. Phys Rev A **17**, 531–541

Olson R.E., Watson R.L., Horvat V. and Zaharakis K.E. (2002): Projectile and target ionization in MeV u(-1) collisions of Xe ions with N-2. J Phys B **35**, 1893–1907

Oppenheimer J.R. (1928): On the quantum theory of the capture of electrons. Phys Rev **31**, 349–356

Raisbeck G. and Yiou F. (1971): Electron capture by 40-, 155-, and 600-MeV protons in thin foils of mylar, Al, Ni, and Ta. Phys Rev A **4**, 1858–1868

Ribe F.L. (1951): Electron-capture cross sections for protons passing through hydrogen gas. Phys Rev **83**, 1217–1225

Rozet J.P., Stephan C. and Vernhet D. (1996): ETACHA: a program for calculating charge states at GANIL energies. Nucl Instrum Methods B **107**, 67–70

Rutherford E. (1924): The capture and loss of electrons by alpha particles. Philos Mag **47**, 277

Ryufuku H. (1982): Ionization, excitation, and charge-transfer for impacts of H^+, Li^{3+}, B^{5+}, C^{6+}, and Si^{14+} ions on atomic-hydrogen. Phys Rev A **25**, 720–736

Sauter F. (1931a): Über den atomaren Photoeffekt bei grosser Härte der anregenden Strahlung. Ann Physik **401**, 217–248

Sauter F. (1931b): Über den atomaren Photoeffekt in der K-Schale nach der relativistischen Wellenmechanik Diracs. Ann Physik **403**, 454–488

Schiff L.I. (1981): *Quantum mechanics*. McGraw-Hill, Auckland

Schlachter A.S., Stearns J.W., Graham W.G., Berkner K.H., Poyle R.V. and Tanis J.A. (1983): Electron capture for fast highly charged ions in gas targets: An empirical scaling rule. Phys Rev A **27**, 3372–3374

Schnopper H.W., Betz H.D., Delvaille J.P., Kalata K. and Sohval A.R. (1972): Evidence fo radiative electron capture by fast, highly stripped heavy ions. Phys Rev Lett **29**, 898–901

Schultz D.R., Reinhold C.O., Olson R.E. and Seely D.G. (1992): Differential cross sections for state-selective electron capture in 25-100-keV proton-helium collisions. Phys Rev A **46**, 275–383

Shakeshaft R. (1979): Relativistic effects in electron capture from a hydrogenlike atom by a fast-moving bare ion. Phys Rev A **20**, 779–786

Shevelko V.P., Rosmej O., Tawara H. and Tolstikhina I.Y. (2004): The target-density effect in electron-capture processes. J Phys B **37**, 201–213

Shevelko V.P., Stohlker T., Tawara H., Tolstikhina I.Y. and Weber G. (2010): Electron capture in intermediate-to-fast heavy ion collisions with neutral atoms. Nucl Instrum Methods B **268**, 2611–2616

Shevelko V.P., Tolstikhina I.Y. and Stöhlker T. (2001): Stripping of fast heavy low-charged ions in gaseous targets. Nucl Instrum Methods B **184**, 295–308

Sommerfeld A. and Schur G. (1930): Über den Photoeffekt in der K-Schale der Atome, insbesondere über die Voreilung der Photoelektronen. Ann Physik **396**, 409–432

Spruch L. (1978): High-impact-velocity forward charge transfer from high-Rydberg states as a classical process. Phys Rev A **18**, 2016–2021

Stobbe M. (1930): Zur Quantenmechanik photoelektrischer Prozesse. Ann Physik **7**, 661–715

Stöhlker T., Kozhuharov C., Mokler P.H., Olson R.E., Stachura Z. and Warczak A. (1992): Single and double electron-capture in collisions of highly ionized decelerated Ge ions with Ne. J Phys B **25**, 4527–4532

Tawara H., Kato T. and Nakai Y. (1985): Cross sections for electron capture and loss for positive ions in collisions with atomic and molecular hydrogen. At Data Nucl Data Tab **32**, 235–303

Thomas L.H. (1927): On the capture of electrons by swiftly moving electrified particles. Proc Roy Soc **114**, 561

Tolstikhina I.Y. and Shevelko V.P. (2013): Collision processes involving heavy many-electron ions interacting with neutral atoms. Physics-Uspekhi **56**, 213–242

Toshima N., Ishihara T. and Eichler J. (1987): Distorted-wave theories for electron capture and the associated high-energy behavior of cross sections. Phys Rev A **36**, 2659–2666

Vogt H., Schuch R., Justitiano E., Schulz M. and Schwab W. (1986): Experimental test of higher-order electron-capture processes in collisions of fast protons with atomic hydrogen. Phys Rev Lett **57**, 2256–2259

Weng M.S., Schinner A., Sharma A. and Sigmund P. (2006): Primary electron spectra from swift heavy-ion impact: Scaling relations and estimates from modified Bohr theory. Europ Phys J D **39**, 209–221

Wentzel G. (1926): Zur Theorie des photoelektrischen Effekts. Z Physik **11**, 574–589